Graduate School Form 30
(Revised 08/14)

# PURDUE UNIVERSITY
## GRADUATE SCHOOL
## Thesis/Dissertation Acceptance

This is to certify that the thesis/dissertation prepared

By Allen Chacha

Entitled
FUNCTIONAL DISSECTION OF ERD14 PHOSPHORYLATION-DEPENDENT CALCIUM BINDING ACTIVITY

For the degree of Master of Science

Is approved by the final examining committee:

Stephen Randall

John Watson

Andrew Kusmierczyk

To the best of my knowledge and as understood by the student in the Thesis/Dissertation Agreement, Publication Delay, and Certification/Disclaimer (Graduate School Form 32), this thesis/dissertation adheres to the provisions of Purdue University's "Policy on Integrity in Research" and the use of copyrighted material.

Stephen Randall

Approved by Major Professor(s): _____

_____

Approved by: Simon Atkinson 12/05/2014

Head of the Department Graduate Program Date

# FUNCTIONAL DISSECTION OF ERD14 PHOSPHORYLATION-DEPENDENT CALCIUM BINDING ACTIVITY

A Thesis

Submitted to the Faculty

of

Purdue University

by

Allen R Chacha

In Partial Fulfillment of the

Requirements for the Degree

of

Master of Science

December 2014

Purdue University

Indianapolis, Indiana

I dedicate this to my parents who have been there for me with their love and support through these challenging two and a half years.

Thank you very much for believing in me.

# ACKNOWLEDGEMENTS

I would like to thank Dr. Randall for the tremendous amount of guidance and patience he has shown me and everyone in the lab. I would also like to thank Dr. Watson for insightful questions during lab meetings that helped improve my project and expand my knowledge of my project. I would also like to thank Dr. Kusmierczyk for serving on my committee and offering insightful feedback. I would like to thank the biology department for the opportunity to earn my masters at IUPUI and all the assistance they have provided me in accomplishing it. Finally, I would like to thank Yuji Yamasaki, Gage Koehler and Jennifer Robison for their help, friendship, and support in the lab.

TABLE OF CONTENTS

Page

Page

# LIST OF TABLES

Table Page

# LIST OF FIGURES

Page

Page

# LIST OF ABBREVIATIONS

| | |
|---|---|
| AA/aa | Amino acid |
| ABA | Abscisic acid |
| ABF | Abscisic response factor |
| ABRE | ABA-responsive element |
| ADH | Alcohol dehydrogenase |
| AREB | Abscisic acid responsive element binding protein |
| Asn/N | Asparagine |
| Asp/D | Aspartic acid |
| At | *Arabidopsis thaliana* |
| ATP | Adenosine Tri-Phosphate |
| bp | Base pair |
| BSA | Bovine Serum Albumin |
| $Ca^{2+}$ | Calcium ion |
| CAMTA | Calmodulin-binding transcription factor |
| CBF | C-repeat/dehydration responsive element binding factor |
| CK2B | Casein Kinase II Buffer |
| CK2E | Casein Kinase II Enzyme |
| CKII | Casein kinase 2 |
| cm | Centimeter |
| COR | Cold-regulated genes |
| CRT | C-repeat |
| CRT/DRE | C-repeat/dehydration responsive element |
| C-terminus | Carboxyl-terminus |
| $Cu^{2+}$ | Copper ion |
| DHN | Dehydrin |
| DI | Deionized |
| DNA | Deoxyribonucleic acid |
| DRE | Dehydration response element |
| DREB | Dehydration responsive element-binding protein |
| DTT | Dithiothreitol |
| *E. coli* | *Escherichia coli* |
| ERD | Early response to dehydration |
| ERD | Early Response to dehydration |
| Glu/E | Glutamic acid |

| | |
|---|---|
| GST | Glutathione S-transferase |
| HSP | Heat shock protein |
| ICE | Inducer of CBF expression |
| kb | Kilobases |
| KO | Knockout |
| LEA | Late embryogenesis abundant protein |
| LP/RP | Lower primer/Right primer |
| min | Minute |
| mM | Millimolar |
| mRNA | Messenger RNA |
| MW | Molecular weight |
| ng | Nano gram |
| N-terminus | Amino-terminus |
| °C | Degree Celsius |
| PBS | Phosphate buffered saline |
| PCR | Polymerase chain reaction |
| PI | Protease Inhibitor |
| pI | Protein isoelectric point |
| RAB | Responsive to abscisic acid |
| ERD | Early response to dehydration |
| ROS | Reactive oxygen species |
| RT | Room temperature |
| SDS-PAGE | Sodium dodecyl sulfate polyacrylamide gel electrophoresis |
| Ser/S | Serine |
| SSB | SDS-PAGE Sample Buffer |
| T-DNA | Transferred DNA |
| Thr/T | Threonine |
| UP/LP | Upper primer/Left primer |
| UTR | Untranslated region |
| v | Volume |
| wt | Weight |
| WT | Wild-Type |
| α- | Antibody |
| µL | Micro litter |
| µM | Micro molar |

# ABSTRACT

Chacha, Allen R. M.S., Purdue University, December 2014. Functional Dissection of ERD14 Phosphorylation-Dependent Calcium Binding Activity. Major Professor: Stephen Randall.

Drought and cold conditions are among the major factors affecting plant growth and crop production globally. Dehydrins are group II late embryogenesis abundant (LEA) proteins characterized by a conserved K-region (EKKGIMDKIKEKLPG consensus sequence) that accumulate in many plants during drought, low temperature, and high salinity to confer stress tolerance. While it has been demonstrated that overexpression of dehydrins improves cold tolerance in various crop plants, the mechanism leading to cold tolerance is still unclear. Previous studies reported phosphorylation of AtERD14 dehydrin by casein kinase II (CKII) led to an increase in calcium binding activity. Mass spectroscopy analysis determined that the phosphorylation was localized to a poly-serine (S) region. To further characterize the S-region, GST fused ERD14 mutants were created via site-directed mutagenesis and deletion of either the amino or carboxyl ends of ERD14 via the QuickChange® Multi Site-Directed Mutagenesis Kit. Phosphorylation of purified mutant proteins by CKII was analyzed via gel shift and direct phosphorylation assays. The effect of phosphorylation on calcium binding activity was also analyzed.

Results showed the serine (S) residue at position 83 was crucial to phosphorylation-dependent molecular mass shift and $Ca^{2+}$-binding activities followed by the serine residue at position 85 in importance. Mutation of serines at positions 83, 84, and 85 completely eliminated the phosphorylation-dependent gel shift and calcium binding. Examination of truncation mutants determined the N-terminal was an important region for protein structure modification and phosphorylation ability leading to $Ca^{2+}$ activation. Calcium binding activity of the truncated mutants indicated the calcium binding site was localized in the region between the S-region and the K-region near the C-terminal end. To characterize the acidic dehydrins contribution to cold tolerance *in vivo*, three single (erd10, erd14, cor47) knockouts (KOs) were characterized. Single KOs produced no cold sensitive phenotype indicating the need for multiple dehydrin KOs in Arabidopsis in order to potentially produce a cold sensitive phenotype.

# CHAPTER 1. INTRODUCTION

One of the major differences between animals and plants is that plants are immobile, they cannot move away from stressful environments such as cold areas. Crop plants exposure to abiotic stresses is among the major agricultural problems facing the world, resulting in more than 50% productivity losses and societal suffering in parts of the world (Boyer et al., 1982; Chen et al., 1994; Bray et al., 2000; Qin et al., 2011). Abiotic stress studies show a series of morphological, physiological, biochemical and molecular changes that adversely affect plant growth and productivity (Levit et al., 1980; Palta et al., 1989; Wang et al., 2000).

Osmotic stresses induced by drought, high salt, and cold temperatures is one of the primary contributor to the decreased crop yields, contributing to over 50% of most major crop loss worldwide (Qin et al., 2011). Osmotic stress can be described as failure to maintain cellular fluid equilibrium when exposed to the surrounding environment. Some plants possess biological capability to withstand low temperature such as in temperatures below -20°C. Membrane integrity and protein stability are among critical functional areas necessary for plant survival (Uemura et al., 2006).

Considerable research has been dedicated to understanding responses of model plants to abiotic stresses. The world population is estimated to exceed 9 billion people by 2050 according to United Nations (UN) estimates. The Food and Agricultural Organization (FAO) estimates over 800 million people world-wide live without enough food. Faced with a rapidly multiplying population, Understanding the stress tolerance mechanisms is important for improving agriculture, particularly, understanding dehydrins has potential to move us a step closer towards smart engineering of crop plants such as cold resistant soybeans (Hume and Jackson, 1981), with better stress tolerance attributes.

Dehydrins are a family of proteins known to play an important role in the cold acclimating process. Central to this thesis is AtERD14 dehydrin that can be phosphorylated strongly by CKII and the phosphorylation event results in significant increase in $Ca^{2+}$ binding activities compared to other Arabidopsis acidic dehydrins (ERD10 and COR47) (Alsheikh et al., 2005). Cold acclimation is a process of interest because understanding acclimation mechanisms has potential to revolutionize agriculture worldwide leading to biotechnological improvements of cold sensitive crop plants to tolerate cold conditions better and allow access to previously inaccessible temperature zones for particular crop plants.

## 1.1 Cold stress and acclimation

Cold stress can be classified as chilling (0 – 15$^{o}$C) and freezing (below 0$^{o}$C) stresses .It is estimated 42% of earth's land has temperatures below -20°C (Ramankutty et al., 2008). To adapt to cold stress some plants have evolved various mechanisms to protect their critical biological functions necessary for survival (Smallwood & Bowles, 2002; Mahajan & Tuteja, 2005; Alsheikh et al., 2005).

In accordance to their cold responsive abilities, plants can be divided into three groups (Pearce et al., 1999; Thomashow et al., 1999; Sharma et al., 2005). First are plants that are susceptible and damaged by temperature below 12°C. Second are plants that are can acclimate to temperatures below 12°C but unable to survive freezing temperatures. Third are plants that are freeze tolerant and able to acclimate to survive temperatures significantly below freezing temperature. Although, actual tolerance levels are dependent on the species, developmental stage and duration of the cold stress. Plants such as spinach and Arabidopsis, originating from temperate climates exhibit an ability to increase their cold tolerance when exposed to cold stress (Thomashow et al., 1999). For instance, *A. thaliana* can survive in -10°C temperatures after acclimating in chilling temperatures whereas unacclimated Arabidopsis fail to survive in -10°C (Gilmour et al., 1988).

The term cold acclimation was first used to describe animals in the 1950s before associating it with plants in the 1960s (Kenefick et al., 1963). Cold acclimation allows plant biological capability to withstand drought or low temperature conditions (Kenefick et al., 1963; Chen et al., 1994). Cold acclimation results in formation of two distinct

effects, first one being cell performance improvement at low temperatures and second effect is an increase in freezing resistance (Kacperska et al., 1989). Acclimation leads to a variety of morphological, physical and biochemical changes of cell membrane fluidity via changes in lipid composition and expression of non-enzymatic proteins that can alter the freezing point (Levitt et al., 1980; Thomashow et al., 2001; Jan et al., 2009). At a cellular level, plant cells go through molecular, physical and structural rearrangements in their macromolecules to minimize freezing induced cellular damage during cold stress. For example, in rye, cold acclimation increases freezing tolerance by preventing expansion induced lysis and formation of hexagonal II phase lipids in membranes. There are a variety of biological mechanisms known to contribute to the development of cold tolerance in plants (Miura and Furumoto, 2013) include:

I. Modulation of membrane lipid composition to increase unsaturated fatty acid content.
II. Induction of cryoprotectants and osmolytes synthesis
III. Antioxidant synthesis
IV. Synthesis of chaperones
V. Synthesis of anti-freeze proteins
VI. Metabolism regulation via enzyme regulation

## 1.2 Cold induced effects on plasma membrane

Studies on cold stress show the event imposes injury on cellular physiology and results in metabolic dysfunction and loss of membrane fluidity resulting in abnormal cellular division and plant growth (Levitt et al., 1980; Palta et al., 1989; Mahajan & Tuteja, 2005). Two factors are considered as contributing to membrane damage under cold stress. The first factor the occurrence of specific freeze-induced lesions associated with the plasma membrane (Steponkus et al., 1993; Uemura and Steponkus, 1999). An increase in phospholipid proportions is the most notable observation seen during lipid composition changes in early cold acclimation stages. Chilling sensitivity correlated with the content of unsaturated fatty acids. Cold sensitive plants have increased saturated fatty acids in phosphotidyl-glycerol in membrane whereas cold tolerant plants contain increased levels of unsaturated fatty acids, mainly in phosphotidylcholine and phosphotidylethanalamine (Hara and Tarashina, 2003). Transgenic tobacco with increased levels of unsaturated fatty acids, had enhanced cold tolerance (Murata et al., 1992; Kodama et al., 1994).

The second factor is lipid peroxidation which can cause a decrease in membrane fluidity and loss of function. (Barclay & McKersie, 1994). Peroxidized membrane and formation of free radicals caused by cold exposure lead to a loss of unsaturated fatty acids and an increase in membrane rigidity, a higher-phase transition temperature, and membrane degradation (Alonso et al., 1997).

The dehydrating effect of extracellular ice crystals is usually the dominant biophysical force exerted on cell membranes at sub-zero temperatures. When temperature drops

below 0°C, freezing injury starts by ice crystals formation in the intercellular spaces (Burke et al., 1976; Chen et al., 1994; Browse & Xin, 2001). Ice crystals usually stay on the outside of the cell as long as the plasma membrane remains intact (Levitt et al., 1980). Compromised plasma membranes allow ice crystals to decrease water potential outside of the cell and osmosis forces water out of the cell (Levitt et al., 1980; Webb & Steponkus, 1993).

There are three major types of membrane damage namely Expansion-induced lysis (EIL), Lamellar-to-hexagonal-II phase transitions (HII) and Fracture-jump lesions (FJL).

### 1.2.1 Expansion Induced lysis

Under freezing stress cells undergo osmotic contraction resulting in surplus plasma membrane folding inside the cell. The surplus membrane ends up creating endocytic vesicles to allow the main plasma membrane to maintain adequate tension (Thomashow et al., 1999; Uemura et al., 2006). On thawing, the endocytic vesicles fail to reincorporate back into the main plasma membrane resulting in protoplast lysis during the osmotic thawing phase.

### 1.2.2 Loss of osmotic responsiveness with lamellar-to-hexagonal II ($H_{II}$) transitions (LOR-$H_{II}$)

Under severe dehydration cellular volume is significantly decreased causing loss of osmotic responsiveness during thawing period. The loss is caused by lateral phase separations and formation of lamellar-to-hexagonal-II phase transitions in areas where the plasma membrane is in close proximity to internal membranes (chloroplast envelope and tonoplast), leading to destabilization of the plasma membrane and ion gradient as the cell loses considerable amounts of water to the external ice (Gordon-Kamm and Steponkus, 1984a; Uemura et al., 1995; Webb et al., 1994).

### 1.2.3 Loss of responsiveness with fracture jump lesions (LOR-FJL)

Freeze induced dehydration in cold acclimated plasma membrane can result in formation of extrusions on the membrane instead of endocytic vesicles in order to mitigate any lysis injury (Gordon-Kamm and Steponkus 1984b). Upon thawing, osmotic expansion usually occurs due to the membrane extrusions ability to reincorporate back into the plasma membrane unlike EIL. Freezing injury in cold acclimated cells occur as loss of osmotic responsiveness associated with fracture jump lesions characterized by deviations of plasma membrane fracture plane as observed under freeze-fracture electron micrographs (Fujikawa and Steponkus 1990; Steponkus et al., 1993).

## 1.3 Cold stress sensory mechanism

To date it is still unclear of the identity of low temperature plant sensors except that studies indicate the presence of multiple primary sensors. Reduction in plasma membrane fluidity is believed to act as sensor to low temperature effects and the membrane rigidification can be sensed and is hypothesized to represent potential injury site (Horvath et al., 1998; Orvar et al., 2000; Martinieire et al., 2011; Knight & Knight, 2012; Wasteneys & Galway, 2003).

The cytoskeleton interacts with plasma membrane and it is known to have an important role in cold signaling and acclimation. Cytoskeleton reorganization is predicted to be a link between membrane rigidification and $Ca^{2+}$ ion influx through the plasma membrane and the vacuole into the cytosol, a key component for the induction of cold regulated (COR) genes (Knight et al., 1996; Orvar et al., 2000; Sangwan et al., 2002). Additional abiotic factors leading to elevated cytosol $Ca^{2+}$ include touch, hyperosmotic, oxidative stress, and UV radiation (Sanders et al., 1999; Sanders et al., 2002; Frohnmeyer et al., 1999; Knight et al., 2000; Knight and Knight, 2001). Influx of $Ca^{2+}$ often cause transmission of signals downstream by means of calcium binding proteins to ultimately alter cellular functions (Knight et al., 1996; Sanders et al., 1999; Trewavas, 1999; Mithofer and Mazars, 2002; Gao et al., 2004).

Steponkus & Lynch, 1989 demonstrated one of the key roles of calcium-induced cellular metabolites was to stabilize cell membranes against freezing injury. Furthermore, calcium supplementation has been observed to positively affect freezing tolerance in plants (Percival et al., 1999). Beyond signaling, calcium is an essential nutrient

requirement for cell wall strengthening, and for maintaining membrane stability and permeability (Roux and Slocum, 1982). Calcium deficiency renders plants weak to pathogens and abiotic stresses, and can lead to impaired root function and plant growth (Conway et al., 1987).

### 1.4 Regulation of gene expression in response to low temperature

Cold acclimation involves precise regulation of transcription factor expression and stress responsive effector genes such as COR genes (Thomashow et al., 1999; Seki et al., 2001; Seki et al., 2002; Kreps et al., 2002; Xiong et al., 2002; Shinozaki et al., 2003). There are two gene groups that exhibit distinct temporal expression patterns in response to low temperatures (Fowler & Thomashow, 2002; Seki et al., 2002). The first group are cold inducible genes that exhibit rapid and short-lived expression in response to low temperature responsive elements of the signal transduction pathway. The second group are genes that gradually increase during cold exposure and these genes directly participate in cellular protection (Fowler & Thomashow, 2002; Seki et al., 2002; Heino & Palva, 2003; Vogel et al., 2005; Van Buskirk & Thomashow, 2006).

Many cold accumulating proteins share common properties such as hydrophilicity, resistance to heat denaturation and contain repeated amino acid sequence regions. These properties are thought to enable these proteins to protect cells against freezing injuries by stabilizing both proteins and membranes during cold stress.

### 1.4.1 Pathway leading to cold tolerance

Abiotic stress responses utilize common pathways. In a cold tolerant plant such as *A. thaliana*, the (abscisic acid) ABA-dependent and ABA-independent pathways activate many stress tolerance genes, including dehydrins genes. The expression of the dehydrin family of proteins is crucial for plant adaptation to severe environmental conditions (Close et al., 1997). Plasma membrane rigidification induces up-regulation of cold-responsive (COR) genes (Orvar et al., 2000) mainly responsive through the ABA independent pathway (Medina et al., 1999; Shinozaki et al., 1997; Shinozaki et al., 1994). Dehydrin genes often contain ABRE elements (ACGTGG/TC) as well, allowing these genes to respond to both the ABA dependent and ABA independent pathways (Narusaka et al., 2003).

## 1.5 Dehydrins ($Y_nS_nK_n$)

The most common way plants combat water stress involves accumulation of late embryogenesis abundant (LEA) proteins (Hanin et al., 2011) via ABA dependent and independent pathways (Medina et al., 1999; Shinozaki et al., 1997; Shinozaki et al., 1994). LEA proteins are often expressed during later stages of seed development and in response to stimuli from abiotic stresses (Hundertmark & Hincha, 2008). Dehydrins were first characterized in cotton during the late stages of embryogenesis and were initially called LEA proteins (Dure et al., 1989).

Dehydrins are group 2 LEA (LEA II) proteins that commonly accumulate in late stages of embryo development and in vegetative tissues in response to environmental stresses associated with low temperature, dehydration and drying stage during seed maturation (Close et al., 1997). Dehydrins do not share any significant sequence similarity with any other proteins found in protein databases (Svensson et al., 2000). The overexpression (OE) of *A. thaliana* (Puhakainen et al., 2004), strawberry (*Fragaria spp*.) (Davik et al., 2013), and wheat (Gramineae) (Houde et al., 1992) dehydrins have demonstrated there is a direct correlation with plant's ability to respond and develop tolerance towards a particular abiotic stressor/s. In particular, when *A. thaliana* transgenics overexpress COR47 and RAB18 dehydrin, they exhibit a higher cold tolerance capability (75 – 85% survival rate) compared to wildtype Arabidopsis (18 – 22% survival rate) (Puhakainen et al., 2004).

### 1.5.1 Dehydrin characteristics

Dehydrins are primarily characterized as proteins containing at least one copy of a 15 amino acid long rich in lysine sequence (K-region) [EKKGIM(E/D)KIK(I/E)KLPG] (Close et al., 1997; Nylander et al., 2001; Hanin et al., 2011). The K-region is a highly conserved region and dehydrins can contain multiple copies of the region (Figure 1) (Close et al., 1997). The K-region sequence is a predicted A2 amphipathic α-helix, a structure known to interact with hydrophobic and polar/non-polar interfaces (Close et al., 1997; Segrest et al., 1990). The hydrophilic and low hydrophobic amino acid

content of dehydrins implicate a flexible structure that does not form a characteristic hydrophobic core typical in folded proteins (Eriksson and Harryson, 2011)

Dehydrins may also contain a tyrosine (Y)-region [(V/T)D(E/Q)YGNP] located near the N-terminus (Close et al., 1997). Another conserved region is a serine (S)-region (LHRSGS4-10(E/D)3) usually located near the N-terminal end (Close et al., 1997; Hanin et al., 2011). This region can be phosphorylated by kinases *in vivo* and *in vitro* (Alsheikh et al., 2003; Alsheikh et al., 2005). The phosphorylation event in some dehydrins has been observed to have a direct correlation on binding of ions such as calcium on the dehydrins (Alsheikh et al., 2003).

Dehydrins can be classified in accordance to the number of conserved domains ($Y_nS_nK_n$) (Alsheikh et al., 2005). The five structural subgroups arising from conserved regions are $K_n$, $SK_n$, $K_nS$, $Y_nK_n$, and $Y_nSK_n$ (Hanin et al., 2011). Furthermore, dehydrins can be categorized according to their isoelectric points (PIs) namely acidic (4.6 – 6.4), neutral (7.2 – 7.6) and basic (8.9 – 9.9) (Danyluk et al., 1994; Koehler et al., 2007). Plants can contain multiple dehydrin genes. For instance, in Arabidopsis, there are 10 known dehydrins (Figure 1), 8 in rice, and 13 in barley (Koehler et al., 2007; Choi et al., 1999; Sterky et al., 2004; Wang et al., 2007; Hundertmark and Hincha, 2008).

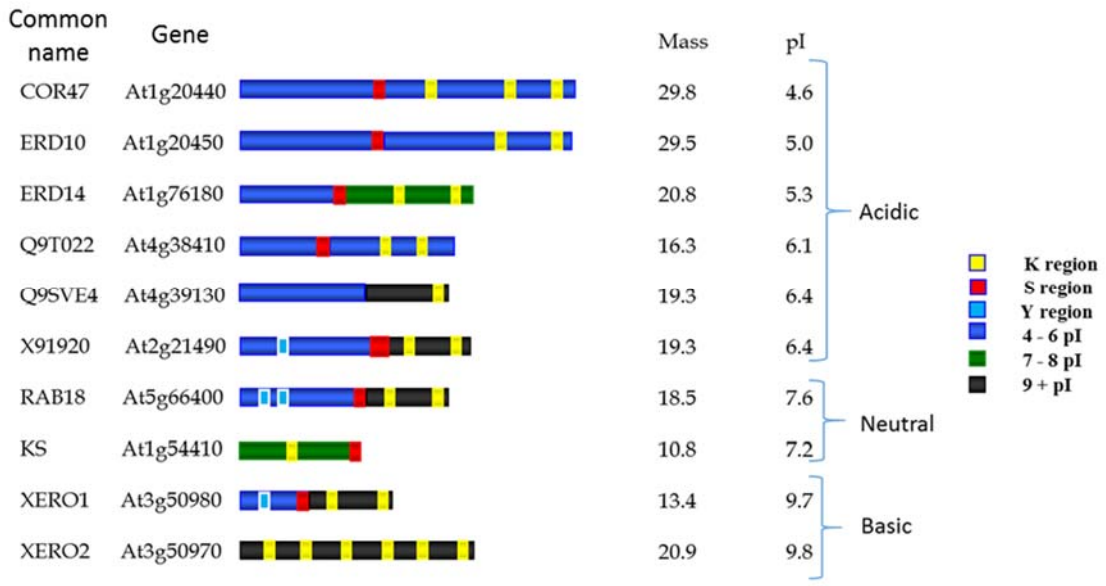


Figure 1. Arabidopsis, dehydrin structures: regions, molecular weight, isoelectric points (pI) (Adopted from Koehler, Phytochemistry 2007).

#### 1.5.1.1 Intrinsically disordered characteristic of dehydrins

The majority of the disordered proteins bind to cellular targets and the interaction induces a folded structure that switches the function of the protein on and off (Dunker et al., 2002; Wright and Dyson, 2009). Disordered proteins are known to assume a fixed structure in order to interact with their targets such as proteins, membranes, RNA, DNA, and metal ions. Majority of known disordered proteins are involved with regulation, signaling or control (Uversky et al., 2005; Dunker et al., 2008). The change of a disordered protein to its functional state is associated with an increase in structure (Uversky, 2005). Disordered proteins appear to indicate an inverse

relationship between protein function (presence of secondary structures) and the random coil content of the protein (Uversky et al., 2005).

In pure form, dehydrins assume a largely disordered random coil structures (Lisse et al., 1996; Ismail et al., 1999; Hanin et al., 2011). According to circular dichroism, proton NMR and solid state NMR analysis, dehydrins are considered intrinsically disordered with a minor (2%) inclusion of α-helices (Lisse et al., 1996; Ismail et al., 1999; Soulages et al., 2003; Bokor et al., 2005; Mouillon et al., 2006). Intrinsically disordered proteins lack a defined 3D structure under physiological conditions (Dunker et al., 2002; Fink et al., 2005; Uversky et al., 2005). The disordered property gives dehydrins ability to stay soluble even after boiling but makes it impossible to crystallize them (Svensson et al., 2000; Livemois et al., 2009).

## 1.6 Dehydrin functions

### 1.6.1 Ability to interact with membranes

Dehydrins have an ability to interact with both proteins and lipids. Interaction between dehydrins and membranes is hypothesized to stabilize membrane integrity during a stressful event. Dehydrins are predicted to have an ability to protect plant cells against dehydration by means of their random coil structures which are predicted to maintain protein structure and bind water (Close et al., 1996).

Certain dehydrins such as maize DHN1 can only be found at membrane surfaces (interact with small unilamellar vesicles) while others (ERD10 and ERD14) have been observed to interact with phospholipid liposomes, suggesting dehydrins have specific functions involving membranes/lipids (Danyluk et al 1998; Koag et al., 2003; Koag et al., 2009; Kovacs et al., 2008). The dehydrin K-region is thought to be responsible for dehydrin/membrane interactions that alter membrane shape composition leading to dehydrin protective functions. The K-region present in most dehydrins is similar to a lipid-binding class A2 amphipathic α-helical structure found in apolipoproteins and α-synucleins (Davidson et al., 1998). One of the roles of the A2 amphipathic α-helical structure is hydrophobic interactions with membranes and denatured proteins (Segrest et al., 1990). Cowpea (*Vigna unguiculata*) and citrus (*Citrus unshin*) CuCOR19 dehydrin studies discovered these dehydrins could form amphipathic α-helices under sodium dodecyl sulfate treatment (Ismail et al., 1999).

During cell dehydration, dehydrin K-regions have been hypothesized to assume an amphipathic α-helical conformation (Hanin et al., 2011). A2 amphipathic α-helix allows for both hydrophilic and hydrophobic interactions to stabilize proteins in water stress environments (Kosová et al., 2007; Ochoa-Alfaro et al., 2012). A2 amphipathic α-helix studies indicate the helix structure aligns negative charges opposite the hydrophobic face and positive charges at the polar/non-polar face (Segrest et al., 1990; Close et al., 1997). The α-helices are hypothesized to bind to intracellular molecules such as membranes and proteins, mainly by hydrophobic interactions (Close et al., 1997) and may serve as a region of interaction for peripheral membrane proteins (Sankaram &

Marsh, 1993). Such interactions were predicted to protect functions of membranes and proteins by preventing aggregation during an osmotic stress event (Hoekstra et al., 2001). Maize DHN1 K-regions were discovered to play a crucial role in interacting with anionic phospholipid vesicles and the interaction was observed to induce further α-helix secondary structure in the presence of liposomes (Segrest et al., 1990).

The K-regions are thought to bind with surfaces of partially dehydrated proteins, biomembrane surfaces, and other K-regions located on the same dehydrin also assuming α-helix formation. When peptides containing multiple K-regions interact, there was an increase in amphipathic nature of α-helices, improving interactions with proteins and plasma membranes (Hanin et al., 2011). Once dehydrin is bound to other proteins, amphipathic α-helical conformation is observed to increase allowing it to protect other proteins (Hanin et al., 2011). Previous studies have also observed random coils have an ability to interact with water which could lead to the stability of proteins or membranes by maintaining water content in dehydrated cells (Ingram & Bartels, 1996; Koag et al., 2003). AtERD10 and AtERD14 proteins have been observed to accumulate on cold acclimated *A. thaliana* plasma membranes. It is hypothesized that plasma membranes can utilize hydrophilic proteins such as dehydrins to support increasing activity of plasma membrane calcium ATPase during cold hardening (Hellergren et al., 1983; Sutinen et al., 1992).

#### 1.6.1.1 Amphipathic α-helix characterization

Amphipathic α-helix is a secondary structure with an opposing polar/non-polar surfaces oriented along the long axis of the helix (Segrest et al., 1990). α-helix is usually formed by repetitive Hydrogen bonds between the carboxyl and amine backbones located four residues apart (Segrest et al., 1992). Amphipathic helices can be grouped into 7 classes namely A, C, G, H, K, L, and M.

Class A amphipathic α-helices represent lipid associating amphipathic helices of apolipoproteins (proteins that bind lipids forming lipoproteins for transportation) found on plasma membranes. A unique feature of class A amphipathic helix is the clustering of positively charged residues at the polar/non-polar surface whereas the negatively charged residues cluster at the center of the polar face. They are mainly involved with transportation of water-insoluble lipids on the plasma membrane but some also have been observed to have metabolic functions via membrane receptor interactions (Segrest et al., 1990).

Class A can be further subdivided into two subclasses of apolipoproteins. The first apolipoprotein subclass are those capable of moving from one lipoprotein to another (A1, A2, A4, C1, C2, C3, and E). Numerous studies support that amphipathic α-helices are responsible for the lipid-associating properties of the exchangeable apolipoproteins (Segrest et al., 1990). A distinctive feature of exchangeable apolipoproteins is the presence of internal 11-amino acid residue repeats that sometimes can duplicate to a 22-amino acid residue amphipathic α-helix (Fitch, 1977). Class A2 amphipathic α-helices associated with dehydrin K-region random coil structure belong to this particular group.

The second subclass are those apolipoproteins that remain with one lipoprotein from synthesis stage to breakdown of that protein (B100 and B48) (Segrest et al., 1990).

### 1.6.2 Ability to bind to metals

When water moves out of the cell, solutes and ions increase in concentration to a level where they can cause damage to the cell by increasing production of reactive oxygen species (ROS). Dehydrins have an ability to bind metals and consequently help decrease ionic concentration (Alsheikh et al., 2003; Alsheikh et al., 2005; Hara et al., 2005; Hanin et al., 2011). Dehydrins have been demonstrated to bind metal ions such as Fe2+, Fe3+, Cu2+, Mn2+, and Zn2+ (Dure et al., 1989; Svensson et al., 2000; Alsheikh et al., 2003; Alsheikh et al., 2005; Hara et al., 2004; Xu et al., 2008). The metal binding property can allow dehydrins to behave like antioxidants since decreasing ion buildup contributes to decreasing prevalence of ROS (Eriksson and Harryson, 2011). Citrus CuCOR15 was discovered to have metal binding activity ($Fe^{3+}$, $Co^{2+}$, $Ni^{2+}$, $Cu^{2+}$ and $Zn^{2+}$) with $Cu^{2+}$ (up to 16 ions) showing the highest affinity (Dure et al., 1989). CuCOR15 can reduce metal toxicity in cells under water stress, a phenomenon known as radical scavenging (Dure et al., 1989). $Fe^{2+}$ binding activates the castor bean (*Ricinus communis*) iron transport dehydrin protein (ITP) to participate in iron transport (Kruger et al., 2002). Further examples are the arabidopsis ERD14, ERD10, COR47 and celery VBA45 dehydrins involvement in $Ca^{2+}$ binding in response to phosphorylation action by kinases (Heyen et al., 2002; Alsheikh et al., 2003; Alsheikh et al., 2005).

### 1.6.3 Ability to behave like chaperones

Dehydrins can function as chaperones, preventing proteins from degrading or refolding them into stable conformation after stress-induced denaturation. Chaperone function is also supported by the known roles of known intrinsic disorder proteins play in cells (Eriksson and Harryson, 2011). Kovacs et al., 2008 study showed dehydrins potentially could prevent thermal-induced protein aggregation and chemical-induced protein denaturation. This chaperone activity was correlated with intrinsically disordered, charged regions in the dehydrin. AtERD10 and AtERD14 dehydrins both exhibit chaperone like activity and show an ability to protect protein substrates from denaturing under heat stress (Kovacs et al., 2008). Protective abilities of ERD14 and ERD10 in Kovacs et al., 2008 study, showed they had better protein protection than the protective capability of Heat Shock Protein 90 (HSP90; eukaryote chaperone) in various assays. The two dehydrins prevented heat induced denaturation of proteins such as firefly luciferase and citrate synthase. (Kovacs et al., 2008).

### 1.6.4 Ability to improve freezing tolerance

Dehydrins show cryoprotective activity towards freezing sensitive enzymes. Dehydrin cryoprotective properties for freeze-sensitive enzymes was demonstrated in citrus (Hara et al., 2001), peach (Wisniewski et al., 1999) and spinach (Kazuoka & Oeda, 1994). Peach PCA60 dehydrin could preserve *in vitro* enzymatic activities of lactase dehydrogenase after several freeze-thaw cycles in liquid nitrogen (Wisniewski et al., 1999). Citrus

CuCOR19 dehydrin was shown to protect catalase and lactate dehydrogenase against freezing inactivation (Hara et al., 2001). The major CuCOR19 secondary structures (random coils), have been predicted to play an important role in cryoprotection of freezing sensitive enzymes. Low temperature causes loss of oligomeric protein function by inducing subunit dissociation. This dissociation can be reduced through interaction with random coiled regions of protective proteins.

### 1.6.5 Ability to scavenge radicals

During stressful events, plants produce an increased amount of reactive oxygen species (ROS) that can cause a decrease in photosynthesis, increase cellular ion leakage, and increase programmed cellular death (O'Brien et al., 2012). ROS are chemically active molecules that can cause a decrease in photosynthesis, increase electrolyte leakage, and increase apoptosis (O'Brien et al., 2012). Lipid peroxidation involves a free radical-mediated degradation pathway that includes polyunsaturated fatty acids resulting in formation of lipid radicals (Hara et al., 2003). Dehydrins contribute to decreased ROS by acting in addition to metal binding activity discussed earlier, by acting directly as *ROS* scavengers (Hara et al., 2004; Ibrahim et al., 2008). The citrus dehydrin *CuCOR15* and Arabidopsis dehydrins (AtERD14, AtERD10 and AtCOR47) were found to bind to ions such as $Fe^{3+}$, $Ca^{2+}$, $Co^{2+}$, $Ni^{2+}$, $Cu^{2+}$, $Zn^{2+}$ (Dure et al., 1989; Alsheikh et al., 2003). By binding metal ions, dehydrins prevent the synthesis of new *ROS* (Hara, 2005; Rorat et al., 2006). Citrus CuCOR19 enhanced membrane cold tolerance in transgenic tobacco plants and

prevented *in vitro* peroxidation of liposomes that could lead to formation of lipid radicals harmful to biological functions (Hara et al., 2003).

CuCOR19 can directly scavenge for hydroxyl and peroxyl radicals are created during cellular dehydration (Hara et al., 2003). CuCOR19, hydroxyl scavenging property assists plants to reduce oxidative damage induced by water stress (Hara et al., 2003).

## 1.7 Dehydrin expression localization

### 1.7.1 Subcellular localization

Dehydrins are primarily localized in the cytoplasm and nucleus (Rorat et al., 2006; Asghar et al., 1994; Goday et al., 1994; Puhakainen et al., 2004) but can be found in various cell compartments such as plasma membrane (Puhakainen et al., 2004; Koehler, unpublished data), mitochondria (Borovskii et al., 2000) and the vacuole (Heyen et al., 2002).

### 1.7.2 Tissue localization

There are two known major Arabidopsis dehydrin groups, those that highly accumulate in seeds (AtCOR47, AtXERO1, atXERO2) and those that are found mostly in vegetative tissues (AtCOR47, AtERD10, AtERD14) especially in vascular tissues (Koehler et al., 2007; Nylander et al., 2001).

Dehydrins can be found in a variety of vegetative tissues with shoot apices showing lowest transcript levels (Koehler et al., 2007). ERD10, ERD14 and RAB18 dehydrins are constitutively expressed in unstressed plants and are localized to vascular tissues of roots, stems, leaves and flowers. Upon stress exposure, there is an increase in dehydrin expression in leaves and shoots compared to unstressed plants (Rorat et al., 2004). XERO2 is absent in unstressed plants and accumulates to detectable levels in stressed plants (Koehler et al., 2007). Acidic dehydrins are present during early stages of seed development although they exhibit a sharp decline in the later stages of seed maturation (Uemura et al., 2006; Orvar et al., 2000; Alsheikh et al., 2003).

COR47, ERD10, ERD14 and Q9T protein sequences are closely related to each other while XERO1, XERO2, RAB18, X91920 protein sequences also show similarity with each other. COR47, ERD10, ERD14, RAB18 and XERO2 transcripts exhibit strong responses to abscisic acid (ABA) during seed imbibition and in young seedlings. Transcripts for acidic dehydrins (COR47, ERD10, ERD14, Q9T022) have been observed to increase 10 to 100-fold during seed imbibition (Koehler et al., 2007).

Acidic dehydrins and XERO2 exhibit similar expression patterns during abiotic stress, with XERO2 exhibiting the greatest increase in response to cold and osmotic stress. These observations suggest dehydrins have distinct roles in seeds and vegetative tissues (Koehler et al., 2007).

## 1.8 Phosphorylation and cold stress

Protein phosphorylation plays a crucial role in many signal transduction pathways and in the regulation of cellular processes (Eriksson and Harryson, 2011). Previous studies indicate low temperatures shift the phosphorylation-dephosphorylation equilibrium to direct signal transduction cascades via cold-specific protein phosphorylation activities leading to cold-specific gene expression that causes protein activity modifications (Teige et al., 2004; Sangwan et al., 2002; Chinnusamy et al., 2007). Studies in rice show that a membrane-associated CDPK is post-translationally activated in response to cold stress (Romeis et al., 2001). Wheat TaADF, induced by cold-stress and phosphorylated by a cold-stress induced kinase is theorized to function in cytoplasmic remodeling by modulating actin depolymerization (Vazquez-Tello et al., 1998). Studies also show that MAPK cascade and dual specificity kinase (peanut STY) can be activated by cold stress (Rudrabhatla & Rajasekharan, 2002; Agrawal et al., 2003).

Phosphorylation modification in dehydrins was first observed in maize DHN1/RAB17 (Plana et al., 1991). A phospho-amino acid study in maize RAB17 (neutral dehydrin similar to AtRAB18) showed S-region specific phosphorylation activities with increased activity observed in embryos exposed to osmotic or dehydration stress (Plana et al., 1991). Arabidopsis acidic dehydrins (AtERD14, AtERD10 and AtCOR47), AtXERO1, celery VCaB45 and rice RAB21 can all be phosphorylated by casein kinase II (CKII) *in vitro* (Eriksson and Harryson, 2011)*;* with the Arabidopsis acidic dehydrins and celery VCaB45 phosphorylation status influenced calcium binding activity of the proteins (Heyen et al., 2002; Alsheikh et al., 2003; Alsheikh et al., 2005).

CKII is a highly conserved serine/threonine protein kinase expressed in most eukaryotic cells. A consensus CKII phosphorylation sequence is Ser/Thr-X-X-Glu/Asp although CKII has also been observed to phosphorylate Tyr at much lower efficiency (Kramerov & Ljubimov, 2012). CKII phosphorylates various targets and regulation of cellular processes such as mobility, cellular differentiation and proliferation (Kramerov & Ljubimov, 2012).

### 1.8.1 Phosphorylation effect on calcium binding activity

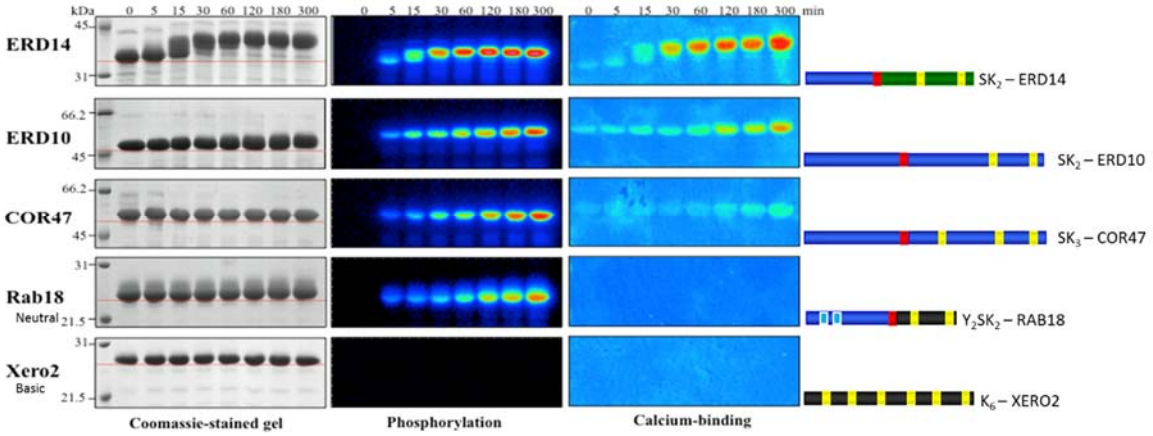


Figure 2. Purified recombinant ERD14, ERD10, COR47, RAB18, and XERO2 treated at 22 °C with CKII for 0–300 min. For [$^{32}$P] phosphorus incorporation, recombinant proteins were in vitro phosphorylated with CKII in the presence of [γ-$^{32}$P] ATP. Calcium-binding activity of E. coli expressed dehydrins was measured by $^{45}CaCl_2$ ligand blotting (Alsheikh et al., 2005).

*In vitro* studies demonstrated three Arabidopsis acidic dehydrins can exist in phosphorylated state in vegetative tissues and the phosphorylation event consequently activate $Ca^{2+}$ binding (Alsheikh et al., 2005). Although RAB18 (neutral dehydrin) is

phosphorylated, this phosphorylation does not result in activation of calcium binding (Figure 2). XERO2 (basic dehydrin) showed no phosphorylation by CKII and shows no calcium binding activity. Competitive inhibition studies of dehydrins show varying binding affinities to other ions but calcium exhibit the highest affinity (Alsheikh, 2005). There is a variation on acidic dehydrins ability to bind to calcium ions with AtERD14 showing the highest binding of $Ca^{2+}$ followed by AtERD10 then AtCOR47 (Figure 2) (Alsheikh et al., 2005). Such observations suggest that acidic dehydrins are functionally distinct from other dehydrins due to their phosphorylation-dependent ion ($Ca^{2+}$) binding activity (Figure 2).

Preliminary results (Moid & Randall, unpublished data) suggested phosphorylation of the S-region is required for calcium binding although it was not known the precise requirements for ion-binding activation.

## 1.9 Hypotheses

ERD14 accumulates following plant exposure to abiotic stress. Preliminary work by Alsheikh, 2005 showed a correlation between phosphorylation-dependent calcium binding activity in ERD14 and phosphorylation of the S-region (by mass spectroscopy analysis) suggesting the S-region is the most likely site for phosphorylation activities. Three hypotheses were generated to characterize AtERD14 and its' S-region.

The first hypotheses predicted the serine region is required for phosphorylation regulated calcium-binding activities. The goal is to determine which amino acids in the S-region are essential for phosphorylation activation of calcium binding. To characterize potential phosphorylation sites, S-region site-directed mutants of AtERD14 were created. Truncation mutants, missing some or all of the conserved regions, were also created. *E. coli* expressed mutants were purified and evaluated for their ability to be phosphorylated by CKII.

The second hypotheses predicted the calcium binding region was localized in the C-terminal half of the ERD14. The goal was to analyze the truncation mutants for the regions crucial for calcium binding.

Thirdly, acidic dehydrins phosphorylation regulated calcium binding was crucial to *in vivo* cold tolerance in Arabidopsis plants. The first goal analyzed 3 acidic dehydrins (erd14, erd10 and cor47) single knockouts (KOs) for a cold sensitive phenotype via cold tolerance electrolyte leakage test. Depending on the first goal outcome, double KOs transgenic plants were to be created to analyze for a cold sensitive phenotype through cold tolerance studies via electrolyte leakage test.

# CHAPTER 2. MATERIALS AND METHODS

## 2.1 Plant Material and Growth Conditions for *Arabidopsis thaliana*

*A. thaliana* (ecotype Columbia) lines (SM.3.40483, SM.3.20259, SM.3.15367) with a multiple independent defective suppressor-mutator transposon insertions (Tissier et al., 1999) in the At1g76180 (erd14), At1g20450 (erd10), and At1g20440 (cor47) genes, were obtained from the Arabidopsis Biological Response Center (ABRC, https://**abrc**.osu.edu/). Single AtERD14 KO, AtERD10 KO and AtCOR47 KO in ecotype Columbia II background seeds were placed on the surface of moistened soil (PRO-MIX) and placed at 4°C for four days stratification in the dark. Plants were grown and fertilized regularly in a Conviron (plant growth chamber) with 6 hour light and 18 hour darkness (short days growth cycle) at 20°C, 59-64% humidity, and light intensity (~100 umol $m^{-2}$s-1 photon flux–LI-COR Quantum model LI-189) using white fluorescent lamps. Plants were generally used four weeks after sowing. For cold tolerance studies, cold treatment was for 7 days at 4°C after which whole plants were tested for electrolyte leakage assays and protein extraction.

## 2.2 Creation of GST-ERD14 substitution mutants

Various substitution point mutations were created by Mohammed Moid, Stephen Randall, Muath Alsheikh, and Don Fish. The ERD14 coding region of DNA was cloned into the bacterial expression vector PET41a as a glutathione S-transferase (GST) fusion protein (Figure 4). To study protein structure function relationships, *in vitro* site directed mutagenesis technology was used to mutate serines in the S-region at specific locus to alanines, the region predicted to be involved in phosphorylation activities. Mutagenesis was accomplished using Strategene QuickChange II Site-Directed Mutagenesis kit and PCR using PfuUltra High Fidelity DNA polymerase. Mutated GST-ERD14 constructs in PET41a were expressed in *E. coli*.

## 2.3 Creation of truncation mutants

Truncation mutants were also created by Tara Sibery, Rafael Tonade, and Stephen Randall. Three truncation mutations of interest were created in addition to substitution mutations. Three Truncation mutations were created using an inverted PCR method where phosphorylated primers controlled DNA synthesis in opposite directions. Primers were created by selecting regions that border the area to be deleted then amplifying the entire plasmid except for the region to be deleted then they were ligated together. The PCR product was transformed into ultra-competent XL-blue *E. coli* cells. Transformed cell colonies were then picked for a plasmid preparation. NaOH-SDS extraction and DNA purification was performed before sequencing the mutants.

The first truncations (T3.0 and T3.5) lacked the distal ($2^{nd}$) carboxy-terminal K-region. Two truncation versions missing the C-terminus were analyzed to determine one with the correct sequence and protein expression. The second truncation (T6.2) was missing all its conserved regions (including S-region) while the carboxy-terminal was intact. The third truncation (T9.6) was missing its amino-terminal sequence with all the conserved regions intact (Figure 5).

## 2.4 Plasmid preparation for sequencing

LB media flasks (100 ml) with 5 µg/µl kanamycin was inoculated with *E. coli* with gene of interest from frozen glycerol stock. The *E. coli* were grown overnight at 37°C on a platform shaker at ~250 rpm. The *E. coli* was then spun at 3500 rpm in GS-6R centrifuge at 4 °C for 15 minutes. The supernatant was discarded and the pellet was resuspended in 6 ml glucose buffer (GTE) containing 5 mg/ml lysozyme and incubated at room temperature (RT) for 5 minutes. DNA was obtained using the standard Alkaline/SDS lysis method (Randall lab protocol). Quality of DNA was confirmed by ideal $A_{260}/A_{280}$ reading between 1.7 – 2.0 ranges. All mutants were confirmed by sequencing (done by Biochemistry Biotech Facility (BBF); http://chem.iupui.edu/research/biochemistry-biotechnology-facility-bbf ) prior to use.

## 2.5 Protein induction

LB media flasks (10 ml containing 50 µg/ml kanamycin) were inoculated with *E. coli* with specific mutant constructs and shaken overnight in 37 °C at ~300 rpm. Fresh LB media (100 ml containing 50 µg/ml kanamycin) were inoculated with overnight cultures (1 ml) and initial absorbance (at 600 nm) reading was determined before shaking the flasks for 2 hours in 37 °C at ~300 rpm. Once *E. coli* cultures reached doubling phase ($A_{600}$ = 0.4), IPTG (1mM final concentration) was added and shaken for further 2 hours. After 2 hours samples were transferred into appropriate centrifuge tubes and spun at 10,000 rpm, 4 °C for 15 minutes. The pellet was resuspended with 50 ml cold DI water and transferred into conical tubes and spun at 3,000 rpm in 4 °C for 20 minutes before storing the pellet in -80 °C. Samples from uninduced (100 µl) and induced (200 µl) samples were boiled in 1X SSB before being separated (10 µl gel load) on SDS-PAGE gel for induction confirmation.

### 2.5.1 Cell breakage for protein extraction

Frozen pellets were resuspended in 0.5X Homogenizing buffer (HMG; 250 mM mannitol, 3 mM EGTA, 25 mM hepes); 1X Roche protease inhibitor cocktail; 1 mM dithiothreitol (DTT). While suspended on ice, the samples were sonicated for 1 minute followed by a minute cooling for a total of 5 minutes with a microprobe (power setting #1, 10% duty cycle for 1 minute then cool on ice for 1 minute). After sonication 1 µl, 1 mM phenylmethylsulfonyl fluoride (PMSF) was added.

The samples were spun for 10 minutes at 10,000 rpm in 4°C, supernatant collected into micro-ultracentrifuge tubes and respun for another 30 minutes in 50,000 rpm. The supernatant was collected and stored in -80°C.

### 2.6 Purification of GST fusion proteins on glutathione agarose resin

While on ice, 40 µl settled volume of suspended GST-bind beads (Invitrogen GST bind resin) were washed three times with 1 ml 1X phosphate buffered saline buffer (PBS; 137 mM NaCl, 2.7 mM KCl, 10 mM $Na_2HPO_4$, 2 mM $KH_2PO_4$, pH 7.4), each time centrifuged at 3000 rpm. The *E. coli* 50,000 rpm supernatants were added (80 µl) and mixed gently and held on ice for 15 minutes. This was followed by addition of 1 ml 1X PBS, mixing and held on ice for 5 minutes. The samples were spun at 3000 rpm for 3 minutes and supernatant discarded. GST-bind beads with bound mutant samples were washed three times with 1 ml 1X PBS. Next, GST-bind beads were washed once with 1 ml 0.5 M Tris-HCl (3 g Tris + 50 ml DI $H_2O$, adjust to pH 7.5 with HCl), followed by 1ml 50 mM Tris-HCl, pH 7.5. Bound proteins were eluted from the GST beads via an elution solution (6 mg glutathione (20 mM final concentration) in 1 ml 50 mM Tris-HCl). Two separate 150 µl elutions were extracted and combined. The samples were separated on SDS-PAGE gel for quality evaluation and quantified via amido black assay.

## 2.7 Protein quantification

An amido black assay (Kaplan, 1985) was utilized to quantitate mutant proteins. Protein samples (10 µl) were pipetted into 13X10 mm labeled test tubes in triplicate including the BSA standards (0 – 40 µg) were diluted with 2 ml DI water. Ten percent (v/v) SDS (0.2 ml) was added and vortexed before adding 0.3 ml 1M Tris/1% SDS (pH 7.5) and mixing the mixture again. Finally, 0.6 ml 104% (w/v) trichloroacetic acid (TCA) was added, vortexed and samples incubated for at least 3 minutes. Samples were filtered onto labeled PROTRAN BA85 millipore filters (0.45 µm pore size) and each filter was washed with 2 ml 6% TCA before air drying them. The samples were transferred into a 1000 ml beaker containing 200 ml amido black staining solution (0.1% (w/v) Amido Black in 50% (v/v) methanol, 10% (v/v) acetic acid) and stirred gently in staining solution for 3 minutes, decanted and rinsed with 200 ml DI water. The filters were destained by washing in 200 ml destaining solution (20% (v/v) methanol, 7.5% (v/v) acetic acid) three more times for 1 minute each. The filters were washed once with 200 ml DI $H_2O$ and blotted with kimwipes on paper towels before cutting out the blue spots and placing them in labeled 16X10 mm test tubes. Finally, 25 mM NaOH/50% (v/v) ethanol was added to all the test tubes and incubated for at least 20 minutes with occasional vortexing before reading the absorbance (630 nm) of the samples on a photospectrometer.

## 2.8 Kinase assay – Gel shift assay

The assay was carried out in microfuge tubes as follows:

Table 1. Gel shift assay protocol showing final concentrations of reagents in a 10 µl reaction volume. CK2B, casein kinase II buffer; PI, protease inhibitor; ATP, adenosine triphosphate; CK2E, casein kinase II enzyme.

| Reaction ingredients | | Volume (µl) | Final Conc. |
|---|---|---|---|
| 10X | CK2B | 1 | 1X |
| 50X | PI | 0.1 | 0.5X |
| 10 mM | ATP | 0.2 | 0.2 mM |
| 500 Units/µl | CK2E | 0.34 | 17 Units/µl |
| Substrate | | X | 2.1 µg |
| Water | | X | |
| Total volume (substrate and water) | | 8.4 | |
| Total reaction volume | | 10 | |

Incubated for 2 hours at 30°C

Reaction stopped with 2X SSB buffer

After the assay, the assay products were separated on 10% SDS-PAGE gel, coomassie stained and imaged via Bio-Rad imager (model GS-670).

## 2.9 Kinase assay – $^{32}P$ incorporation assay

The assay was carried out in microfuge tubes as follows:

Table 2. Gel shift assay protocol showing final concentrations of reagents in a 10 µl reaction volume. CK2B, casein kinase II buffer; PI, protease inhibitor; ATP, adenosine triphosphate; CK2E, casein kinase II enzyme.

| Reaction ingredients | | Volume (µl) | Final Conc. |
|---|---|---|---|
| 10X | CK2B | 1.5 | 1X |
| 50X | PI | 0.3 | 1X |
| 1 mM | Hot/Cold ATP | 3.4 | 0.25 mM |
| (84 µl water, 4.4 µl 20 mM ATP, 1.2 µl 10 µCi/µl $^{32}P$-ϒ-ATP) | | | |
| 50 Units/µl | CK2E | 5 | 17 Units/µl |
| | Substrate | X | 2.1 µg |
| | Water | X | |
| Total volume (substrate and water) | | 4.8 | |
| Total reaction volume | | 15 | |

The reaction was incubated at 30 °C for various times before stopping it with 2X SSB buffer. The assay products were separated on 10% SDS-PAGE gel, coomassie stained and imaged. The gels were dried for two hours before exposing the dried gels to an imaging phosphoscreen overnight. The screen was imaged using the Typhoon 7000 phosphoimager. $^{32}P$ quantification analysis (image J software) was carried out by including both bands that showed phosphorylation activities at ~64 kD due to insufficient resolution.

## 2.10 Protein extraction and quantification

Leaves were isolated from four week old Arabidopsis plants and flash frozen in liquid nitrogen before being stored in -80 °C freezer. Leaf tissue (~1 g) was reduced to a fine powder by grinding with liquid nitrogen-cooled mortar and pestle. Leaf tissues (~0.1 g) were placed in microfuge tubes and boiling 1X SSB buffer was added to the samples at a 1:2, sample to buffer. The mixture was further homogenized via an electric pestle grinder at low speed. The samples were further boiled for 4 minutes and centrifuged at 10,000 rpm for 10 minutes. The supernatant was transferred to a new tube and mixed well to normalize the protein concentration. An aliquot was removed for protein concentration quantification via amido black assay (method 2.6) and the remainder was frozen at -80 °C. Normalization of purified protein samples were sometimes carried out using Imaging Densitometer (model GS-670) in conjunction with Image J software (http://imagej.nih.gov/ij/).

## 2.11 SDS-PAGE and Immunoblotting

After four weeks in 20 °C, wild type Arabidopsis (C907), Erd14, Erd10 and Cor47 single KO plants were transferred to 4°C for 7 days. Whole plant samples from 20 °C and 4 °C were homogenized in 2 volumes 1X SSB buffer and separated by 10% SDS-PAGE gel (Laemmli, 1970).

For immunoblotting, the gel was equilibrated in Western transfer buffer (25 mM Tris, 192 mM glycine, and 20% (v/v) methanol) for 30 minutes. Gels were then transferred

to PROTRAN® BA85 nitrocellulose membrane with 0.45 µm pore size by a transfer overnight at 0.2 Amps at 4 °C. The nitrocellulose membrane was blocked in 1X PBS/5% (w/v) milk (137 mM NaCl, 2.7 mM KCl, 4.3 mM $Na_2HPO_4$, 1.47 mM $KH_2PO_4$/5% Nestle® Carnation instant nonfat dry milk pH to 7.4) for three hours at room temperature (RT) to block non-specific binding sites. Primary antibody (1:10,000 PBS/5% Milk) raised against ERD14, ERD10 or COR47 proteins (Alsheikh, 2005) was incubated for overnight at 4 °C and washed three times with 1X PBS/5% Milk blocking solution for 10 minutes. The secondary antibody (α-rabbit IgG; Sigma Aldrich) conjugated with peroxidase was incubated for 45 minutes at room temperature followed by three 15 minutes washes with 1X PBS/5% Milk blocking solution and then washed twice with 1X PBS for 15 minutes. The blot was gently dried with filter paper and immediately exposed to a chemiluminescent reagent solution (SuperSignal West Dura extended duration substrate) (Pierce Biotech Roadford, IL) for detection of peroxidase activity via Bio-Rad (model GS-670) imager.

## 2.12 Creation of heterozygous knock out lines

Table 3. Single KO acidic dehydrins used for creation of homozygous transgenic lines.

| | | | | Predicted PCR band sizes (base pairs) | |
|---|---|---|---|---|---|
| Genes | Gene # (NCBI) | Line | Insert location | T-DNA | WT |
| ERD14 | At1g76180 | SM.3.40483 | Exon | 800 | 1869 |
| ERD10 | At1g20450 | SM.3.20259 | Exon | 1595 | 1844 |
| COR47 | At1g20440 | SM.3.15367 | Exon | 1350 | 1644 |

Homozygous Erd14, Erd10 and Cor47 single KO transgenic plants were planted and after four weeks, stamens of the transgenic plants were removed and plants were crossed by transferring pollen from one KO plant to the stigma of a different KO plant. For example, using Erd10 pollen to cross with Erd14 stigma and vice versa. The progeny were genotyped to confirm the presence of both genes of interest via PCR method. After transplanting confirmed heterozygous (F1) seeds, these plants were allowed to flower and self-fertilize inside sleeves. Sleeves prevent cross-pollination and ensure self-fertilization. F2 leaf tissues were collected but were not yet genotyped via PCR to find homozygous double knock outs. The seeds (F2) were harvested and are awaiting sowing after confirming a homozygous double knock out line (in progress).

## 2.13 Confirming genotypes for double heterozygous knock out plants

AtERD14, AtERD10, and AtCOR47 knock-out (KO) lines (SM.3.40483, SM.3.20259 and SM.3.15367 respectively) were used to create heterozygous double KOs (Table 3). Four weeks old AtERD14, AtERD10 and AtCOR47 single KO leaf tissues were extracted and DNA extraction was carried out using DNAzol (Invitrogen) protocol with modifications (Randall, 2004 unpublished). To confirm ERD14, ERD10 and COR47 gene disruption PCR products from the wild type and SALK lines were generated using Ex-Taq polymerase (Takara) and primers indicated in table 5. Amplified wild type ERD14, ERD10 and COR47 sequences were predicted to be 1869, 1844 and 1644 base pairs respectively (Table 3). Detection of T-DNA insertion into ERD14, ERD10 and COR47 gene was accomplished using the left border primer sequence and the right primer downstream of the ERD14, ERD10 and COR47. The bands generated from the T-DNA insert were approximately 800, 1595 and 1350 base pairs for Erd14, Erd10 and Cor47 respectively (Table 3).

Thermal cycling was accomplished using an Applied Biosystems 2720 Thermal cycler. The PCR reactions were prepared for sequencing via a QIAquick PCR Purification Kit (Qiagen) using manufacturer instructions. PCR products were analyzed using TAE buffer system and 1% agarose gel electrophoresis (Hoefer Scientific Instrument PS250) at 70 Volts for an hour. The gel was imaged with Bio-Rad (model GS-670) imager.

## 2.14 PCR reactions for genotype analysis

The following ingredients were used for 25 µl volume PCR reactions.

Table 4. Protocol for PCR reaction of single KO genotyping analysis.

| Reagents | 1X reaction (µl) | Final Concentration |
|---|---|---|
| $MgCl_2$ buffer (25 mM) | 2.0 | 2 mM |
| dNTPs (10 mM) | 0.5 | 0.25 mM |
| Upper primer (5 µM) | 1.0 | 0.2 µM |
| Lower primer (5 µM) | 1.0 | 0.2 µM |
| GoTaq (5 u/µl) | 5.0 | 0.025 u/µl |
| Template | X | 60 ng |
| $H_2O$ | X | |

Table 5. The primers, primer size, PCR product band sizes and annealing temperature for genotype analysis of the transgenic lines. TM = annealing temperature; bp = base pairs.

| | |
|---|---|
| SPM32 - Transposon specific primer 29 | 5'-TAC GAA TAA GAG CGT CCA TTT TAG AGT GA – 3' |
| | **ERD10** |
| Upper Primer or SPM32 | ERD10CS108972U: Right 29 bp 65.02 TM AGAAGAAGATTGTTGAAGGAGATCATGTG |
| Lower Primer | ERD10CS108972L: Left 29 bp 64.97 TM AAGCTAGATTGCAGATATTTTTCGGGTAA |
| TDNA primer | SPM32 |
| WT band expected size | 1844 bp |

Table 5 continued

| | |
|---|---|
| T-DNA band expected size | 1595 bp |
| | **ERD14** |
| Upper Primer or SPM32 | ERD14SM340483U: Left 29 bp 65.01 TM<br>GACATCCCATTCTTTAAAATCTCTTTTGC |
| Lower Primer | ERD14SM340483U: Right 29 bp 65.00 TM<br>AATGTTTTGTGATTAGCTGGATCTCATGT |
| TDNA primer | SPM32 |
| WT band expected size | 1869 bp |
| T-DNA band expected size | 800 bp |
| | **COR47** |
| Upper Primer or SPM32 | COR47CS103649U: Left 29 bp 65.00 TM<br>CTCCCACATCATTATTCATTCTTTAACCA |
| Lower Primer | COR47CS103649L: Right 29 bp 64.96 TM<br>CTATTTCCGGGCAAATTATGTAGTGTTTT |
| TDNA primer | SPM32 |
| WT band expected size | 1644 bp |
| T-DNA band expected size | 1350 bp |

## 2.15 Electrolyte leakage assay for cold tolerance studies

Cold sensitive tests were carried out by subjecting 4 weeks old single KO plants to a controlled temperature followed by measurements of electrolyte leakage as indication of tissue damage at that particular temperature over time. Four weeks old Arabidopsis whole plants were harvested and transferred into 16X100 mm glass tubes in an ethylene glycol bath (Brinkman RC20 cooler) pre-cooled to -1.5°C. Plants were kept at -1.5°C for an hour before adding an ice chip to each test tube and maintaining the temperature for another hour. The temperature was then lowered at a 1 degree decrement every two hours. Samples (3 replicates) at each target temperature were removed from the bath and thawed at 4°C overnight followed by incubation with 3 ml water and shaking (250 rpm) for at least 6 hours. Conductivity was measured with a portable conductivity meter (Milwaukee Model MW301 EC meter). One hundred percent electrolyte leakage was measured by the conductivity meter following freezing of the plants at -80°C overnight.

## 2.16 Calcium-ligand blot assay

After carrying out kinase assay, phosphorylated/unphosphorylated samples were separated on 10% SDS-PAGE gels and transferred to polyvinyl difluoride (PVDF) membranes/blots and calcium ligand blots were performed (Maruyama and Nonomura, 1984; Randall, 1992). The blots were washed once with 5 mM ethylene glycol tetraacetic acid (EGTA), pH 7, then washed three times with 60 mM KCl, 2.5 mM $MgCl_2$,

5 mM imidazole, pH 7 buffer. The blots were probed with ~300 µM $^{45}Ca$ (1 µCi $^{45}Ca$/ml) in the previous buffer for 15 minutes.

The blots were washed with 50% (v/v) ethanol for 30 seconds before immediately washing them again in 50% ethanol for 5 minutes. The blots were gently dried and exposed to a phosphoscreen overnight before imaging them with a Typhoon 7000 phosphoimager.

# CHAPTER 3. RESULTS

## 3.1 Mutant constructs were sequenced, induced in *E. coli* and purified.

Alsheikh et al., 2005 data identified the ERD14 S-region as the main phosphorylation site. Substitution mutations were strategically created in amino acid positions within the S-region, predicted to become phosphorylated by CKII. CKII phosphorylates serines/threonines that are 3 residues upstream of an acidic amino acid (E – glutamic acid or D – aspartic acid) residue. To characterize the S-region in detail, GST fused ERD14 mutant constructs created by Tara Sibery, Mohammed Moid, Rafael Tonade, Stephen Randall, Muath Alsheikh, and Don Fish, were sequenced by IU Biochemistry Biotechnology Facility (BBF) and I confirmed the entire coding regions were correct in sequence and orientation (Figure 3 & Figure 4) by alignment comparison with the known ERD14 sequence obtained from TAIR (http://www.arabidopsis.org/)before expressing all the construct proteins (Figure 5 – Figure 7).


➢ T3.5 ERD14 sequence

- MAEEIKNVPEQEVPKVATEESSAEVTDRGLFDFLGKKKDETK PEETPIASEFEQKVHISEPEPEVKHESLLEKLHRSDSSSSSSSEE EGSDGEKRKKKKEKKKPTTEVEVKEEEKKGFMEKLKEKLPGE

➢ T6.2 ERD14 sequence

- MAEEIKNVPEQEVPKVATEESSAEVTDRGLFDFLGKKK DETKPEETPIASEFEQKVHISEPEPEVKHESLLEKLHRSY HPKTTVEEEKKDKE

➢ T9.6 ERD14 sequence

- DSSSSSSSEEEGSDGEKRKKKKEKKKPTTEVEVKEEEKK GFMEKLKEKLPGHKKPEDGSAVAAAPVVVPPPVEEAH PVEKKGILEKIKEKLPGYHPKTTVEEEKKDKE

Figure 3. Truncation mutation model and truncation mutation ERD14 protein sequences. T3.5 has a deleted C-terminus along with one of the K-regions; T6.2 had S and K-regions deleted leaving a partial C-terminus sequence; T9.6 N-terminus was deleted, leaving intact conserved regions downstream. Mutants were created by T. Sibery, R. Tonade and S. Randall (unpublished data).


Figure 4. GST-ERD14 site specific mutation locations. ERD14 represents WT protein. Amino acid residues highlighted in red indicated substitution mutations. Mutants were created by Alsheikh, D. Fish, M Moid, S. Randall (unpublished data).

Before analyzing the mutant constructs, protein expression of the constructs was confirmed. GST-ERD14 mutant proteins were all induced successfully (Figure 5 – Figure 7) and were observed to run at a higher apparent molecular mass than predicted on SDS-PAGE gels (Appendix A1) (Alsheikh et al., 2005). Substitution mutants ran at ~64 kD (predicted mass = ~52 kD) whereas T3.5, T6.2 and T9.6 ran at ~55 kD, ~51 kD, ~51 kD (predicted mass = ~46 kD, 42 kD and 44 kD respectively) respectively. Two versions of truncation/deletion mutant (T3 and T3.5) with a deleted C-terminus including the K-region near the C-terminal end were induced (Figure 6). T3 exhibited extensive

proteolysis while T3.5 mutant version showed no proteolysis effects hence was used for the remainder of the project. Comparing T3 and T3.5 protein sequences (Appendix A6) showed no significant difference in their sequences but the T3.5 expressed at higher levels and appropriate mass. DNA sequence alignment of the two truncations revealed T3 might contain a faulty stop codon leading to instability of the synthesized protein.

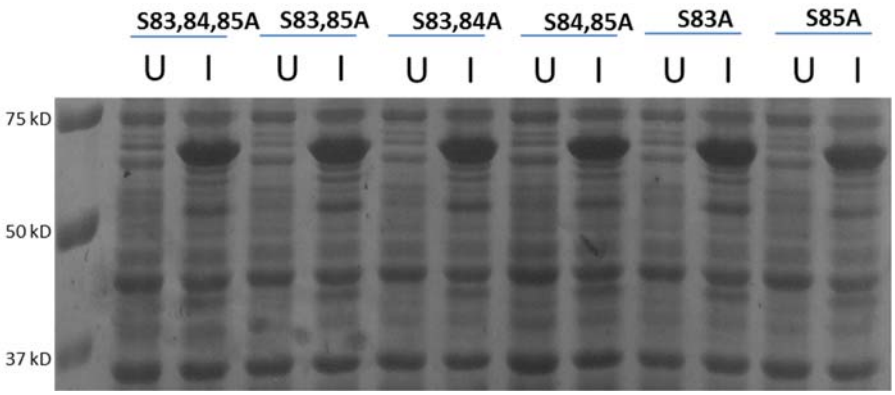


Figure 5. E. coli Induced expression of GST-ERD14 substitution mutants with 1mM IPTG for 2 hours. U = Uninduced, I = Induced. All protein samples (5 µl load) were separated on 10% SDS-PAGE. Substitution mutation samples ran at ~64 kD.

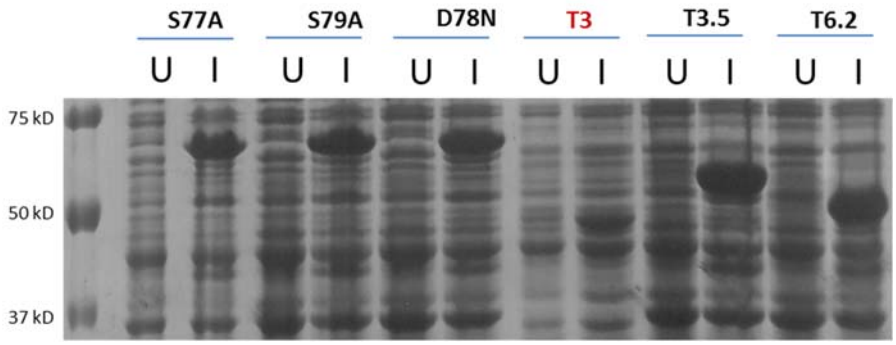


Figure 6. E. coli Induced expression of GST-ERD14 substitution mutants with 1 mM IPTG for 2 hours. U = Uninduced, I = Induced; D = Aspartic acid; N = Asparagine; T = truncated mutant. All protein samples (5 µl load) were separated on 10% SDS-PAGE. Substitution mutation samples ran at ~64 k; T3 mutant rant at ~48 kD; T3.5 ran at ~55 kD; T9.6 ran at ~51.

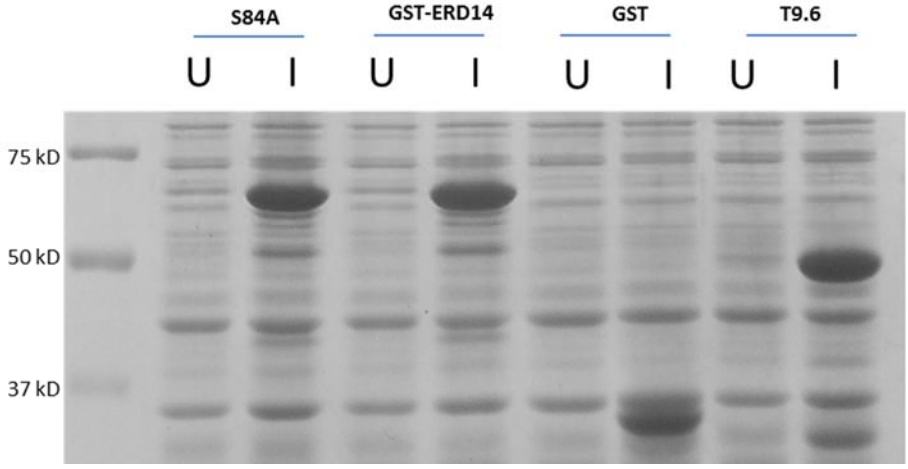


Figure 7. E. coli Induced expression of GST-ERD14 S84A substitution mutant, GST-ERD14, GST and T9.6 truncation mutant with 1 mM IPTG for 2 hours. U = Uninduced, I = Induced; D = Aspartic acid; N = Asparagine; T = truncated mutant. Substitution mutations ran at ~64 kD; GST ran at ~35 kD; Substitution mutation samples ran at ~64 kD; T9.6 ran at ~51 kD.

All GST-ERD14 mutant constructs in pET41a plasmid were purified on the GST bind resin (Figure 8). Purified samples were quantified via amido black assay (Table 6) and SDS-PAGE lanes were all loaded with 3.75 µg protein (Figure 8). Truncation mutant T3.5 was separated on a separate SDS-PAGE gel not shown in the current results but also ran larger than predicted (Appendix A1). Two bands were isolated from purified T9.6 mutant, a heavy band (~51 kD) and light band (~35 kD) which was absent in all other constructs (Figure 8).

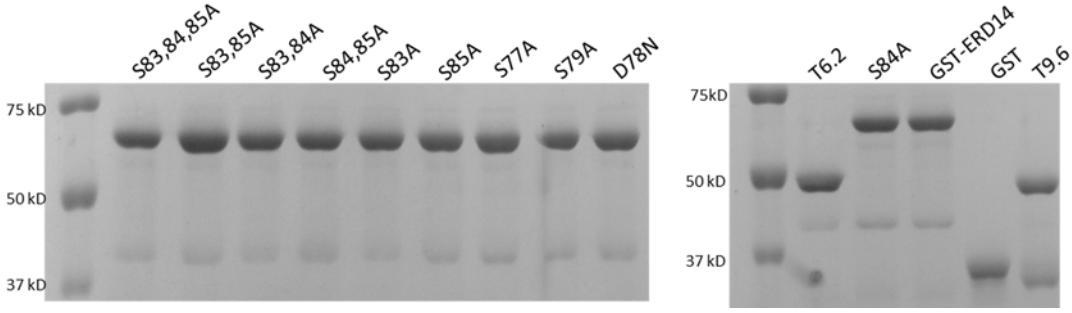


Figure 8. Purified GST-ERD14 mutant proteins loaded at 3.75 µg on the SDS-PAGE gel. GST fused ERD14 mutant samples were purified on GST bind resin before quantifying the samples via amido black assay. Protein quantity were estimated to be within 20% range of each other by BIO-RAD densitometer.

Table 6. Amido black protein concentrations used for protein analysis.

| Sample ID | Mutant ID | Amido Black (µg/µl) |
|---|---|---|
| 14 | GST-ERD14 | 0.8 |
| 15 | GST | 1.2 |
| 7 | S77A | 0.4 |
| 9 | D78N | 0.3 |
| 5 | S83A | 0.3 |
| 13 | S84A | 0.3 |
| 6 | S85A | 1.2 |
| 3 | S83,84A | 0.5 |
| 2 | S83,85A | 1.7 |
| 4 | S84,85A | 2.1 |
| 1 | S83,84,85A | 0.5 |
| 11 | T3.5 | 0.8 |
| 12 | T6.2 | 3.1 |
| 16 | T9.6 | 0.3 |

## 3.2 The ERD14 S-region and amino-terminus end are crucial for phosphorylation and calcium binding activities.

AtERD14 was previously observed to be phosphorylated by CKII and consequently the phosphorylation had a positive correlation on calcium binding activities (Alsheikh et al., 2005). Mass spectroscopy analysis (Alsheikh et al., 2005) suggested the S-region as the crucial ERD14 phosphorylation site. One of the goals for my thesis was to identify the portions of AtERD14 and the specific serine residues in the S-region crucial for CKII phosphorylation dependent gel shift, $^{32}P$ incorporation, and calcium binding.

### 3.2.1 Specific serine residues in the S-region are crucial for phosphorylation-dependent gel shifts in ERD14.

Phosphorylation of AtERD14 was demonstrated to cause a shift in apparent molecular weight when separated on SDS-PAGE gel (Alsheikh, 2003 & 2005). Gel shift assays were carried out on all mutant constructs to determine their ability to shift in apparent mass after phosphorylation by CKII.

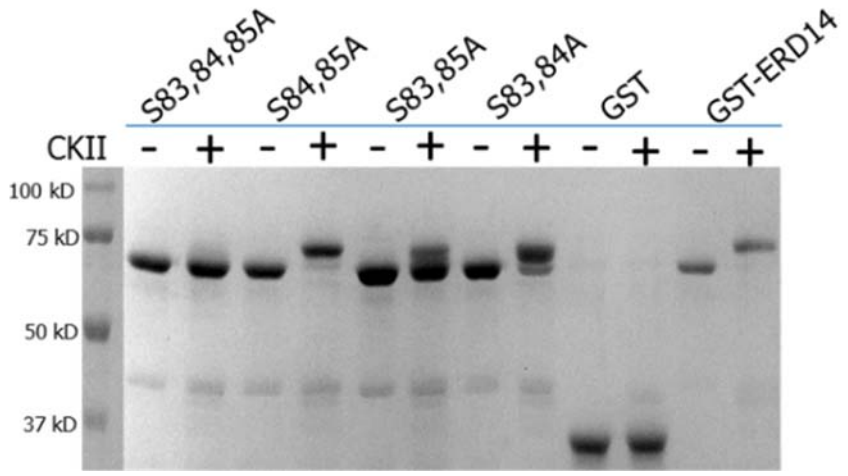


Figure 9. Gel shift assay for GST-ERD14/WT, double and triple mutants. Purified E. coli expressed GST-ERD14 was treated with (+) or without (-) CKII for 2 h at 22 °C. After SDS-PAGE separation, gels were Coomassie stained.

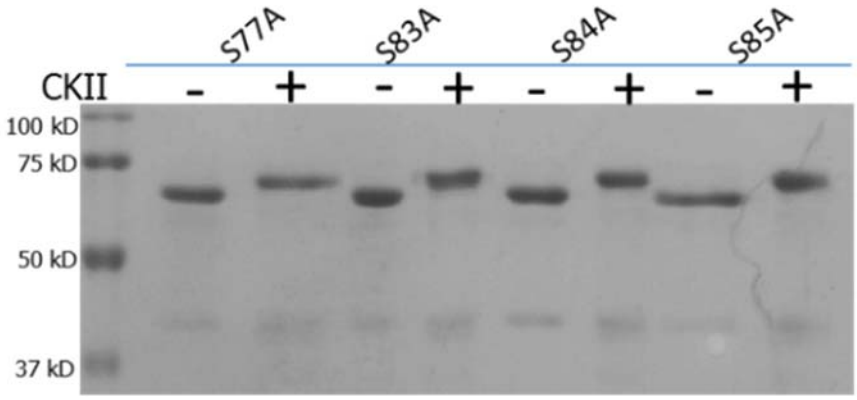


Figure 10. Gel shift assay for GST-ERD14 single substitution point mutants. Purified E. coli expressed GST-ERD14 was treated with (+) or without (-) CKII for 2 h at 22 °C. After SDS-PAGE separation, gels were Coomassie stained.

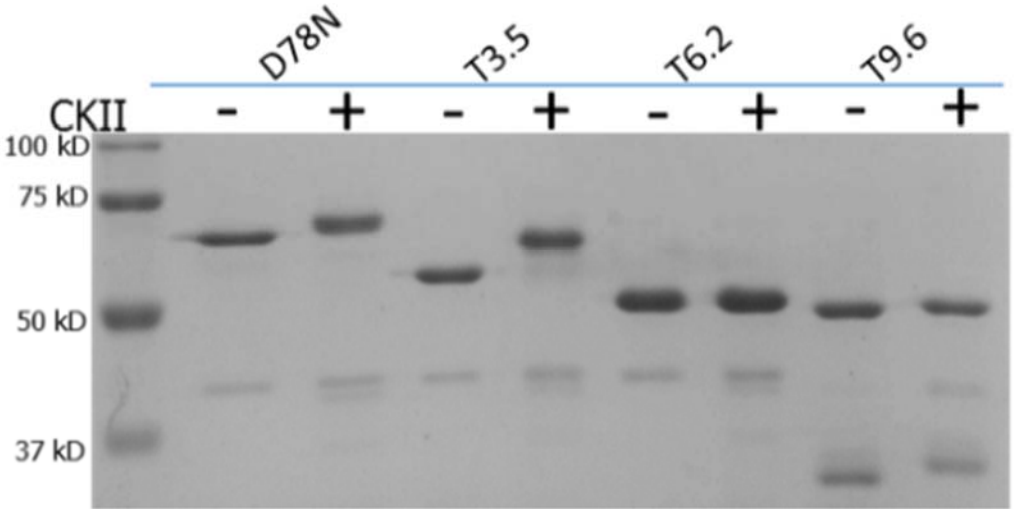


Figure 11. Gel shift assay for truncated mutants and D78N single mutant. Purified E. coli expressed GST-ERD14 was treated with (+) or without (-) CKII for 2 h at 22 °C with or without CKII. After SDS-PAGE separation, gels were coomassie stained.

Table 7. Summary of mutant proteins response to treatment with CKII.

| **Protein showing apparent molecular mass shift after phosphorylation** | **Proteins not showing full shift in apparent molecular mass after phosphorylation** |
|---|---|
| GST-ERD14 (Positive control) | GST (Negative control) |
| S77A | T6.2 |
| D78N | T9.6 heavy band |
| S83A | S83,84,85A (Negative control) |
| S84A | S83,85A |
| S85A | S83,84A |
| T9.6 light band | |
| S84,85A | |
| T3.5 | |

GST-ERD14/WT apparent molecular mass after CKII phosphorylation was ~70 kD while unphosphorylated WT was ~65 kD (Figure 9; Table 7). The GST protein alone showed no mass shifting characteristic and hence ran at ~35 kD before and after CKII treatment (Figure 9; Table 7; Appendix A1). The truncation mutants T6.2 and T9.6 when treated with or without CKII ran at ~51 kD. The truncation mutant T3.5 ran at ~55 kD and at ~60 kD when phosphorylated by CKII (Figure 11; Table 7; Appendix A1). WT, S83A, S84A, S85A and T3.5 exhibited a complete molecular mass shift after phosphorylation by CKII (Figure 9 – Figure 11; Table 7). Mutants S83,84A, S83,85A, S77A and D78N exhibited impaired ability to mass shift compared to WT. The triple (S83,84,85A), T6.2 mutations completely terminated molecular mass shifting capability of GST-ERD14 after CKII phosphorylation (Figure 9 & Figure 11; Table 7). Interestingly, the truncation mutant T9.6 heavy band showed no apparent mass shift but the lighter band showed a shift in molecular weight (Figure 11).

From the gel results, S83A mutation exhibited a gel shift but when paired with a mutation at position 85 (S83,85A), the phosphorylation-dependent mass shift was decreased (Figure 9 & Figure 10). When the serine mutation at position 83 was paired with a serine mutation at position 84 (S83,84A), a gel shift was observed after CKII phosphorylation (Figure 9 & Figure 10). Mutant S84,85A shifted normally after being phosphorylated. The gel shifting results suggest there might be an order of importance in the serine residues (in position 83, 84 and 85) and their ability to influence ERD14 molecular mass shifting properties after CKII phosphorylation. That order of importance seems to be serine at position 83>85>84.


Figure 12. S-Region protein sequence displaying mutations at specific key locations affecting phosphorylation activities.

The GST-ERD14 truncation mutant missing all the "S" and "K" regions (T6.2) and the mutant missing the N-terminal end (T9.6) (Figure 7) showed no mass shift after CKII phosphorylation. The GST-ERD14 truncation mutant (T3.5) (Figure 7) with a deleted C-terminal along with the second K-region (closest to the C-terminal) exhibited a molecular mass shift (Figure 11). It was concluded that a region crucial for phosphorylation-dependent gel shift activities is located in the N-terminal region of the ERD14 protein.

### 3.2.2 The S-region and the amino-terminus are both important for ERD14 phosphorylation.

Phosphorylation of GST-ERD14 constructs were monitored by incorporation of $^{32}P$ from ATP to study their phosphorylation capability *in vitro*. Before carrying out $^{32}P$ incorporation for all mutant samples, GST-ERD14 (WT) and S83,84,85A mutants were first evaluated for the rate of $^{32}P$ incorporation through 5 minutes (300 seconds) (Figure

13). WT was expected to show $^{32}P$ incorporation, GST was predicted to show no incorporation and S83,84,85A due to its lack of mass shifting property observing during gel shifting assays, was predicted to exhibit little $^{32}P$ incorporation.

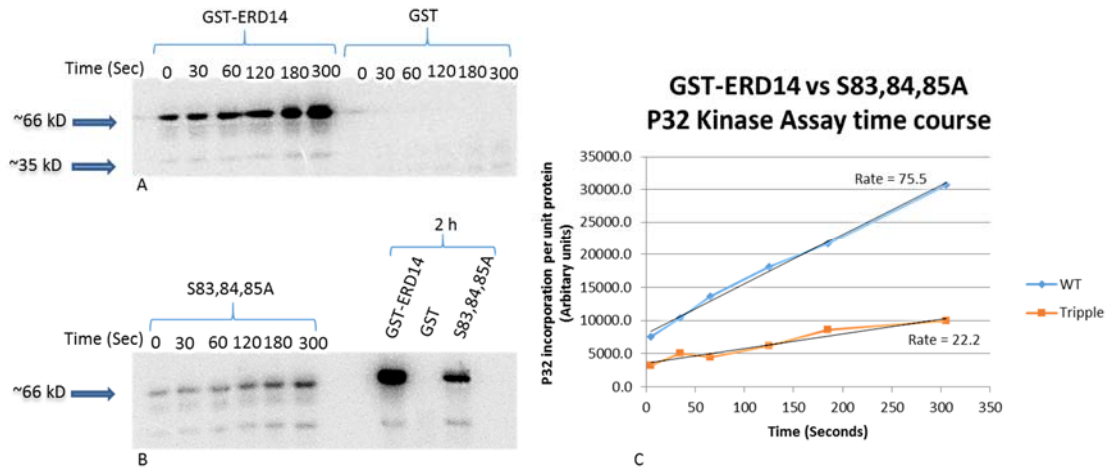


Figure 13. Five minutes $^{32}P$ incorporation kinase assay to determine linear relationship of $^{32}P$ incorporation and time. E. coli-expressed GST-ERD14 (WT), GST, and S83,84,85A mutants were in vitro phosphorylated with CKII in the presence of [ɣ-32P]ATP for 2 h at 30 °C. The reaction starting time was not a true zero time point; it took ~5 sec before the reaction could be stopped. WT phosphorylation rate = 75.5; S83,84,85A phosphorylation rate = 22.2; GST-ERD14 (WT) $R^2 = 0.9948$; S83,84,85A $R^2 = 0.9355$.

The $^{32}P$ kinase assay 5 minute time course experiments lacked a true zero time point. It took ~5 seconds before the first sample reaction could be terminated, allowing for immediate $^{32}P$ incorporation before terminating the reaction. The time course was adjusted by adding 5 seconds to all the data points (5, 35, 65, 125 and 305 seconds respectively).

As seen in figure 13, there was a linear relationship as a progression of time where WT was phosphorylated at a 3-fold (75.5 units $^{32}p$ incorporation/600 sec) faster rate than

S83,84,85A (22.2 units $^{32}$p incorporation/600 sec) (Figure 13). A 2 hour $^{32}$P incorporation kinase assay appeared to exhibit a similar quantitative relationship between WT and S83,84,85A phosphorylation as that observed over 5 minutes time point (Figure 13B). $^{32}$P kinase assays (in four independent experiments) for all ERD14 mutants were carried out for 5 minutes to study the relative $^{32}$P incorporation into all the constructs (Figure 14).

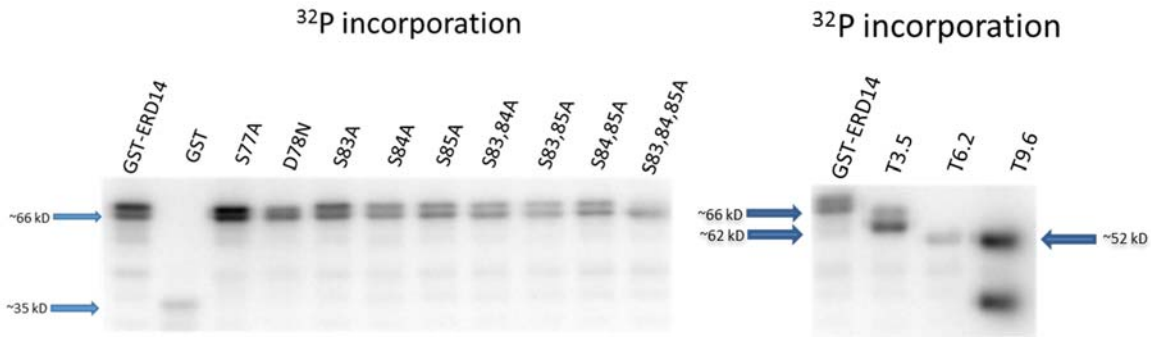


Figure 14. Five minutes $^{32}$P incorporation kinase assay for all mutant constructs. Purified E. coli-expressed GST-ERD14 mutant constructs were in vitro phosphorylated with CKII in the presence of [ɣ-32P]ATP for 5 minutes at 30°C. All substitution mutations ran ~66 kD, GST ran ~35 kD, T3.5 = ~62 kD, T6.2 & T9.6 = ~52 kD.

At a 5 minute reaction time (Figure 14) all proteins showed apparent doublets due to the low 32P incorporation at these short times. WT exhibited increased $^{32}$P incorporation towards its higher mass band while GST showed very little to no $^{32}$P incorporation. S77A, S83A, S85A mutant constructs exhibited strong $^{32}$P incorporation in both its lower and upper mass bands (Figure 14). S83,84A, S83,85A and T6.2 mutants showed a pronounced decrease in $^{32}$P incorporation in both the lower and upper bands,

compared to WT. The triple mutant S83,84,85A exhibited trace amounts of $^{32}P$ incorporation in its lower band and no higher mass band was observed. Truncated mutant T3.5 $^{32}P$ incorporation occurred mostly on its lower mass band. The T6.2 mutant that eliminated apparent mass shifting capability (Figure 11) also appeared to decrease phosphate incorporation onto AtERD14 (Figure 14 & Figure 15). The full-sized truncated mutant T9.6 (~51 kD) showed no molecular mass shifting properties (Figure 11) but was strongly phosphorylated. The lower band (~35 kD) showed apparent mass shifting and was phosphorylated. To account for variability in loading gels, a quantitative estimate of $^{32}P$-incorporation was obtained by calculating the $^{32}P$ incorporated per unit protein quantitated on the same gel. The decrease in phosphate incorporation into AtERD14 seen on D78N, S83,85A, T6.2 correlates with the loss of apparent mass shifting in those particular mutants. The above trends were still observable in a two hour $^{32}P$ incorporation kinase assay blot (Appendix A7). These observations were further analyzed by carrying out a two-tail t-test of the four independent experiments to determine the significance of each mutant construct effect on $^{32}P$ incorporation compared to the WT.

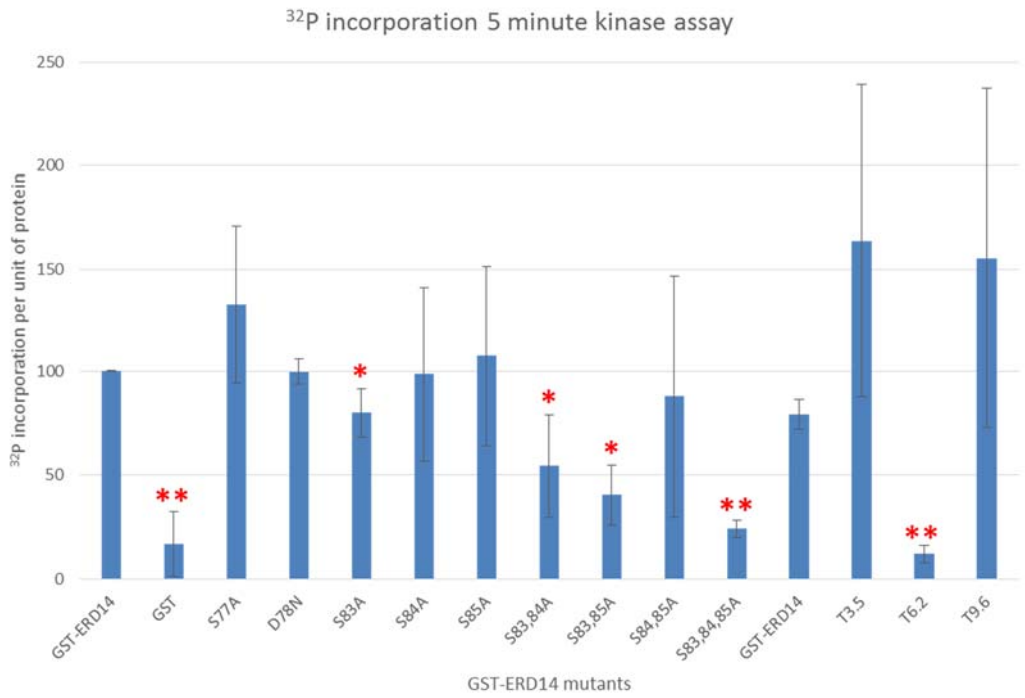


Figure 15. Average $^{32}P$ incorporation into GST-ERD14 mutants at 5 minutes (n = 4), GST-ERD14 and GST. $^{32}P$ incorporated values were divided by the protein values for corresponding lanes for each experiment before averaging the values. Significance difference in values compared to GST-ERD14 were estimated with the students t-test; one star, $p<0.05$; two stars, $p<0.001$.

T-test results further supported figure 14 observations that there was a significant decrease in $^{32}P$ incorporation in GST, S83A (P = .04), S83,84A (P = 0.03), S83,85A (P = 0.002), S83,84,85A (P = 0.00001) and T6.2 (P = 0.00001) mutants compared to the WT (Appendix A3). S77A mutation showed enhanced $^{32}P$ incorporation compared to WT, suggesting that the serine residue at position 77 might play an important role in down regulating phosphate incorporation into ERD14 S-region. Additionally, serines at position 83, 84 and 85 are clearly important for phosphorylation activities on ERD14 protein. The truncated GST-ERD14 mutant missing the S-region and both the K-regions

(T6.2) had trace amounts of $^{32}P$ incorporation comparable to S83,84,85A mutant whereas the two truncated mutants (T3.5 and T9.6) with their S-regions present exhibited strong $^{32}P$ incorporation compared to the construct missing the S-region. In summary, S-region serine residues at position 83, 84 and 85 were important for phosphorylation related mass shift properties of ERD14 and they further played an important role in phosphate incorporation onto ERD14 S-region. Furthermore, the N-terminal end including the S-region were important regions for mass shifting activities related to phosphorylation but the S-region was crucial for phosphate incorporation onto ERD14 protein. This data supports the conclusion that the S-region is a significant phosphorylation site as hypothesized.

### 3.3 The calcium binding region is localized near the amino-terminus half of the ERD14.

It was hypothesized that calcium binding activity was localized in one or all of the three predicted calcium binding sites of AtERD14 (Figure 16). To test this hypotheses, I analyzed the three truncation mutations (Figure 7) and D78N mutant (Figure 6) to localize the region in ERD14 sequence important for calcium binding. AtERD10 and AtCOR47 S-regions both contain asparagine instead of aspartate residue and Alsheikh et al., 2005 demonstrated both these dehydrins bound $Ca^{2+}$ to a lesser extent than AtERD14. Generally, calcium-binding domains contain glycine/proline and acidic/hydroxylated residues (Appendix A5) (Knight et al., 1996). Glycine/proline residues are known to enhance bends in calcium-binding loop regions and sometimes

directly provide carbonyl oxygens for calcium coordination. Though no algorithm predicts a calcium binding domain (eg. EF-hand) in ERD14, a model of possible calcium binding sites in ERD14, based loosely on calcium binding parameters, was created predicting possible calcium binding regions (Figure 16) (Stephen Randall unpublished data).

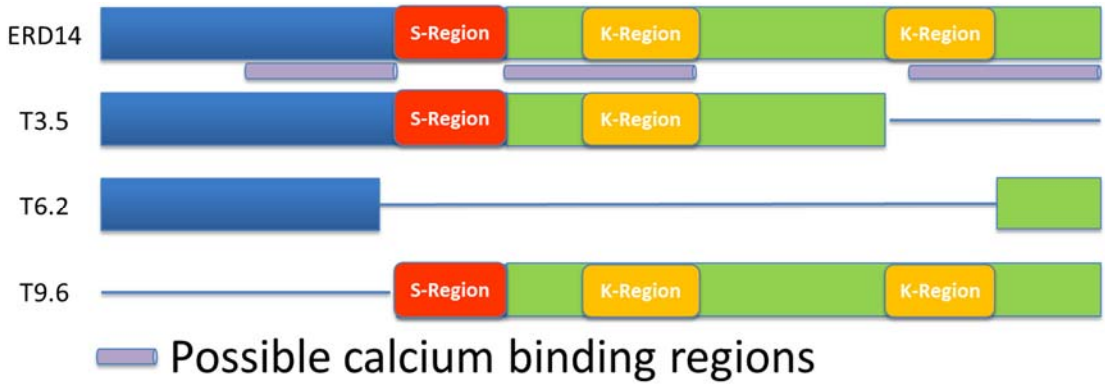


Figure 16. ERD14 protein sequence model exhibiting possible sites for calcium binding activity (By Stephen Randall).

### 3.3.1 The S-region is crucial to $Ca^{2+}$ binding activities.

Calcium binding activities of GST-ERD14 mutants were measured by ligand blot to determine ERD14 site/s crucial to calcium interaction.

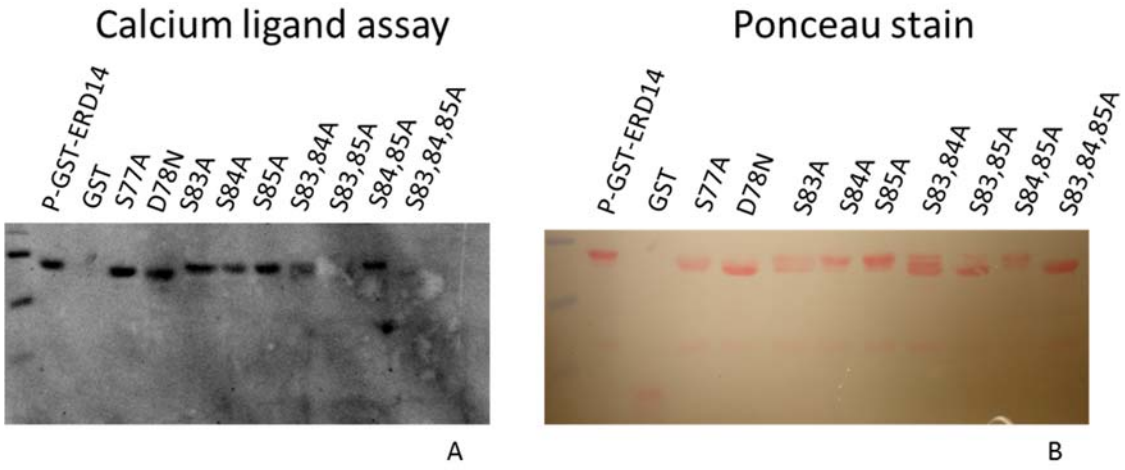


Figure 17. Analysis of calcium binding of point mutations. Purified E. coli expressed GST-ERD14 mutants were in vitro phosphorylated with CKII for 2 h at 30°C. (A) Calcium binding activity of GST-ERD14 mutants was measured by ligand blot. Radioactivity was visualized with a Typhoon 7000 phosphorimager. (B) Calcium blot was subsequently stained with ponceau stain to observe protein amounts on blots.

GST-ERD14 showed calcium binding activity while GST showed no calcium binding activity after phosphorylation by CKII. Except for S83,85A and S83,84,85A, all substitution mutant constructs exhibited calcium binding activity after phosphorylation by CKII (Figure 17). Calcium binding assay on the substitution mutations indicated D78N mutant had no observable effect on calcium binding activity following phosphorylation by CKII. Mutants S83,85A and S83,84,85A exhibited no significant calcium binding activities while S83,84A exhibited a decrease in calcium binding activity. Ponceau stain

of the calcium blot was carried out to visualize the proteins. The stained proteins showed similar mass shift behavior as the gel shift assay (Figure 9 – Figure 11), confirming their phosphorylation status. These observations support the importance of serine residues at positions 83 and 85 in phosphorylation dependent calcium binding activities in ERD14.

### 3.3.2 $Ca^{2+}$ binding activities are localized downstream near the AtERD14 S-region.

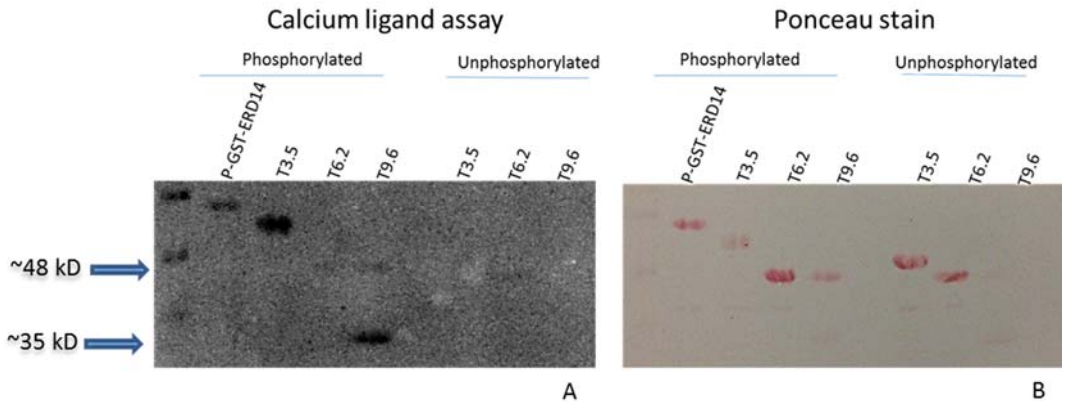


Figure 18. Calcium ligand assay of phosphorylated truncated mutants. Purified E. coli expressed GST-ERD14 was in vitro phosphorylated with CKII for 2 h at 30°C. Calcium blot was subsequently stained with ponceau protein stain. P-GST-ERD14, Phosphorylated GST-ERD14.

As previously observed on gel shift assay results (Figure 9 – Figure 11), using ponceau staining technique on the calcium treated blot, the truncation mutant (T3.5) missing its C-terminal and K-region near the C-terminal end, exhibited a molecular mass shift following phosphorylation with CKII (Figure 11). The truncation lacking the conserved

regions (T6.2) and the one (T9.6) missing the N-terminal end with all the conserved regions still present, lost the ability to mass shift following phosphorylation by CKII (Figure 11). Following calcium ligand assay, truncation mutant T3.5 and T9.6 were observed to have calcium binding activity whereas truncation mutant T6.2 showed no calcium binding activity after phosphorylation by CKII (Figure 14). From $^{32}P$ incorporation results (Figure 14), T9.6 mutant was observed to incorporate $^{32}P$ on both expressed bands (~35 kD & ~52 kD) but on calcium ligand blot assay results (Figure 18), the mutant only showed calcium binding activity on its lower band (~35 kD) with little to no calcium activity on its higher band (~52 kD; circled in red on figure 18).
These observations indicated that the region between the S-region and K-region near the C-terminal end of the ERD14 protein is important for calcium binding which correlates with the second (middle) predicted calcium binding site on the model (Figure 16 & Figure 26).

## 3.4 Single acidic dehydrin KO plants exhibit no significant difference in cold tolerance.

### 3.4.1 Acid dehydrin expression in the single KO erd14, erd10 and cor47.

Before carrying out cold tolerance studies on single exonic KO transgenic plants (Figure 19), the protein expression was evaluated to confirm their successful protein level disruption (Figure 19). To achieve this, whole leaves (from 22°C and 4°C) were extracted and dehydrin protein expression was analyzed by western blot.

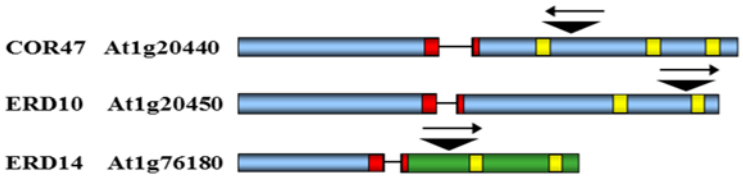


Figure 19. T-DNA Insertion in dehydrin genes of A. thaliana. T-DNA location and orientation are specified with black triangles above dehydrins illustrated. Dehydrin name and chromosome location left of the model. The straight lines represent introns. The S-segment is designated in red. The K-segment is designated in yellow.

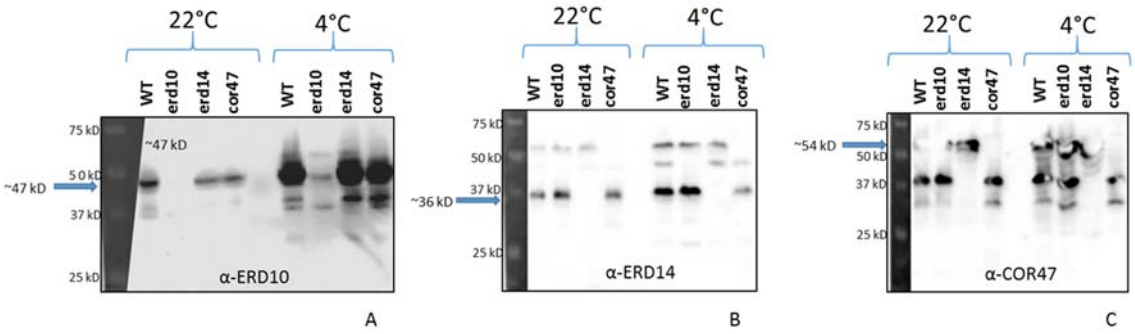


Figure 20. Dehydrin protein accumulation in wild type and KO lines grown at 22 °C and 4 °C. α-Cor47, α-Erd14 and α-Erd10 represent primary antibodies against their designated dehydrins. Four weeks old Arabidopsis transgenic plants acclimated for 7 days at 22 °C or 4 °C on short day growth cycle, were collected and protein extracted via leaf tissues. Proteins were separated on 10% SDS-PAGE gel, transferred onto a nitrocellulose membrane and western blot technique using specific antibodies for cor47, erd14 and erd10. Apparent mass (predicted mass) are erd10: 47 kD (29 kD); erd14: 36 kD (20 kD); cor47: 54 kD (29 kD).

Western blot analysis of the protein expression exhibited successful KO of Erd14, Cor47 and significant knock-down (KD) of Erd10 protein (Figure 20). At 22 °C, there was no detectable dehydrin protein expression in the respective single KOs.

### 3.4.2 Knock out in individual acidic dehydrins show no significant difference in cold tolerance

*In vivo* studies have importance in their ability to allow us to further characterize ERD14 functions in a plant. A cold sensitive phenotype is required to allow us to carry out phenotype rescuing studies with WT and some of the 14 constructs to determine the importance of phosphorylation dependent calcium binding activity on ERD14 and their impact on cold tolerance of *A. thaliana*. To achieve this, single KO erd14, erd10 and cor47 transgenics were analyzed for their ability to produce a phenotype during cold stress.

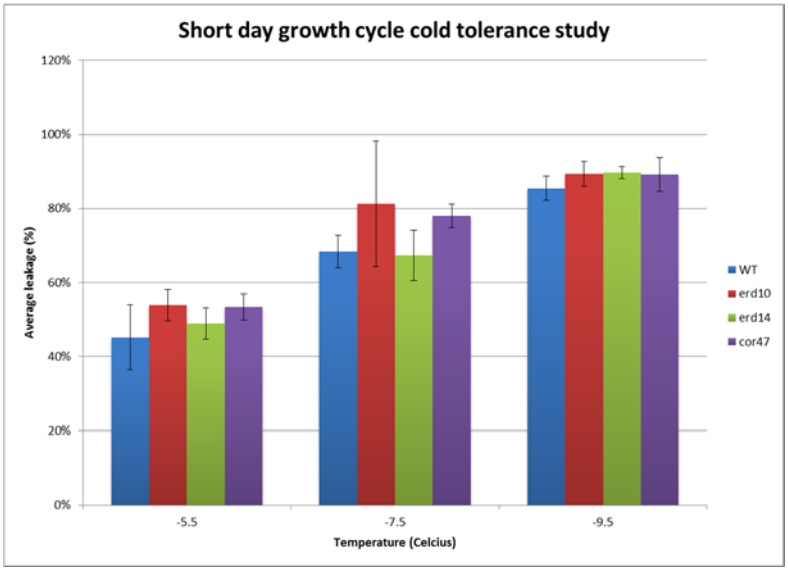


Figure 21. Electrolyte leakage of Arabidopsis WT (C907), erd10, erd14 and cor47 single KOs transgenics at different freezing temperatures on short day growth cycle (6 h light, 18 h dark). 4 week old Arabidopsis transgenic plants acclimated for 7 days at 4 °C. Electrolyte leakage was measured using plants cold treated at -5.5°C, -7.5°C and -9.5°C at a refrigerating rate of 2 °C per hour from -1.0 °C. Columns and bars give the mean ±SE of the 10 experiment repeats.

Once the KOs were evaluated for their protein expression, they were characterized for cold tolerance. The electrolyte leakage analysis revealed the $LT_{50}$ (temperature at which 50% of maximal leakage is obtained) was between -5.5 °C and -7.5 °C. At around -9.5°C the sample tissues were close to 100% cellular electrolyte leakage (considered a measurement of cell death) (Figure 21). A large change in cold tolerance (cellular electrolyte leakage) was observed in the transition between -5.5 °C to -7.5 °C. The electrolyte leakage study showed no significant difference in cold tolerance between *A. thaliana* (WT), erd14, erd10 and cor47 transgenic plants, hence lack of a viable phenotype to move forward with the project.

It is known that many Arabidopsis single KOs fail to exhibit visible, directly informative phenotype, a phenomenon which has been largely linked to prevalence of functional redundancy (Bouche & Bouchez, 2001). Part of the explanation has been linked to high gene duplication frequency and that genes belonging to gene families that share close similarities in their sequences allowing for phenotype rescue from a single KO event (Bouche & Bouchez, 2001). It was concluded that it was necessary to create a homozygous double KO line to search for a viable phenotype to use *in vivo* cold tolerance studies.

### 3.4.3 Creation of heterozygous double KO T1 lines

Failure to detect cold tolerance phenotypes with the single KOs, the second goal was to create homozygous double KOs transgenic lines to search for a line that can produce a phenotype illustrating a deficiency during cold stress exposure. Single KO lines were successfully crossed and PCR reactions confirmed successful insertion of the target genes from paternal line to maternal line.

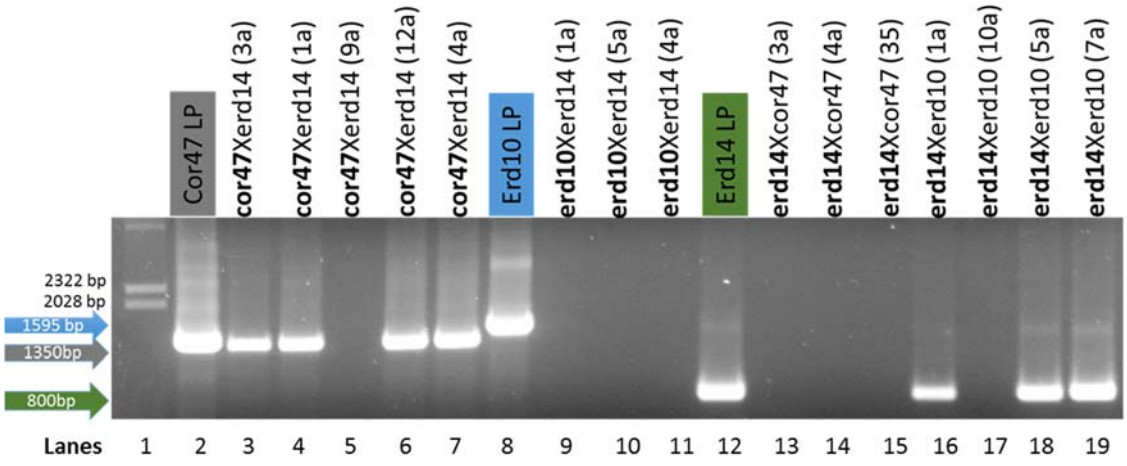


Figure 22. Successful crossing of paternal genes into the recipient plants. Stably expressed single KO homozygous lines were crossed with different single KO homozygous lines to form a heterozygous line that was analyzed by PCR for the presence of paternal copy of KO genes. PCR products were separated on 1% agarose gel. Expected PCR products of paternal KO genes are 800 bp, 1350 bp and 1595 bp for erd14, cor47 and erd10 respectively. Lanes 2, 8 and 12 are positive controls representing single KO homozygous PCR products. Lanes 3 – 7 represent cor47 and erd14 heterozygous line. Lanes 9 – 11 represent erd10 and cor47 heterozygous lines. Lanes 13 – 19 represent erd14 and erd10 heterozygous lines. Bolded dehydrin = paternal gene.

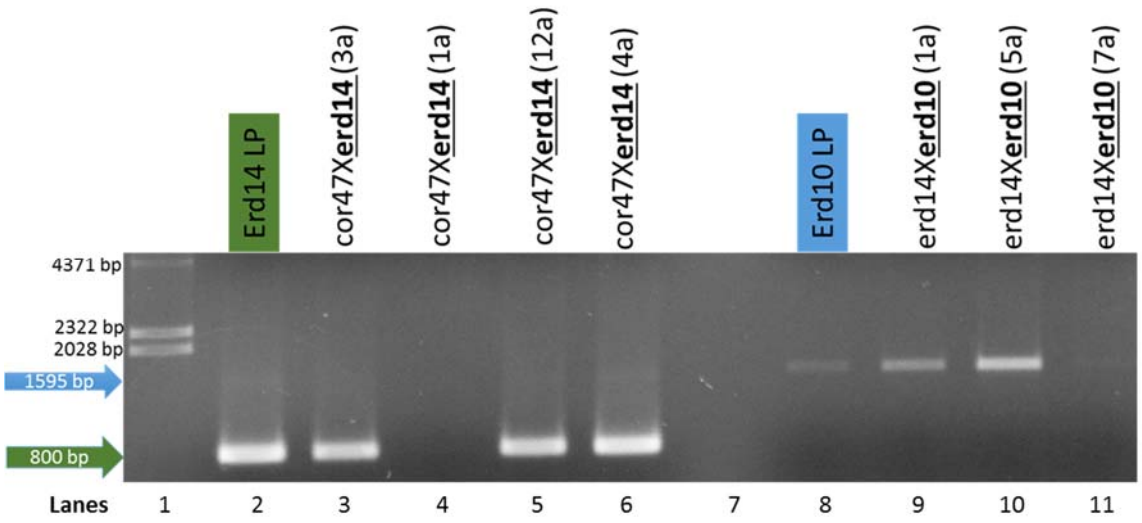


Figure 23. Presence of maternal genes in the recipient lines. Stably expressed single KO homozygous lines were crossed with different single KO homozygous lines to form a heterozygous line that were analyzed by PCR for the presence of maternal gene. PCR products were separated on 1% agarose gel. Expected PCR products of paternal DNA are 800 bp and 1595 bp for erd14 and erd10 respectively. Lanes 2 and 8 are positive controls representing single KO homozygous PCR products. Lanes 3 – 6 represent cor47 and erd14 heterozygous line. Lanes 9 – 11 represent erd14 and erd10 heterozygous lines. Underlined dehydrin = maternal gene.

Two different heterozygous transgenic lines were successfully created, cor47 X erd14 line 1 (4 transgenics) and erd14 X erd10 line2 (3 transgenics) (paternal X maternal genes) (Figure 22 & Figure 23). The Erd10 X erd14 cross failed to produce a successful heterozygous transgenic as indicated by the lack of paternal gene detection by paternal gene primers (Figure 22). Out of the 7 heterozygous lines carrying paternal genes (Figure 22), cor47 X erd14 (1a) and erd14 X erd10 (7a) lines could not be shown to be heterozygotes as indicated by the failure to detect the presence of maternal genes (Figure 23). This could be explained by either PCR reaction failure or a possible mix-up

during the labeling process. Genotyping confirmed five heterozygous (T1) lines (cor47Xerd14 – 3a, 12a and 4a; erd14Xerd10 – 1a and 5a) carrying intact maternal genes (Figure 23) as well as paternal genes (Figure 22).

Two of each T1 lines (cor47Xerd14 (12a), cor47Xerd14 (4a), erd14Xerd10 (1a) and erd14Xerd10 (5a)) were chosen for selfing and 72 samples of each line were planted in order to try to create a homozygous double KO line/s. The T2 plants are awaiting genotyping analysis via PCR in order to locate a successful homozygous double KO line/s.

# CHAPTER 4. DISCUSSION

Alsheikh et al., 2005, demonstrated phosphorylation of AtERD14 had a positive correlation to the proteins' ability to bind calcium and modify its structure. Furthermore, through mass spectroscopy analysis of AtERD14, it was determined the S-region was primary site of phosphorylation activity (Alsheikh et al., unpublished data). I was interested in characterizing AtERD14 and its' S-region further to identify specific serine residues crucial to phosphorylation-dependent structural modification and calcium binding activity. To accomplish this, kinase and calcium binding assays were carried out.

Gel shift assay results indicate the N-terminus of ERD14 protein plays an important role in molecular mass shifting properties brought about by phosphorylation. Deletion mutation results (Figure 14) clearly indicate apparent molecular mass shift is lost in the absence of the N-terminus end of the protein. Consistent with this deletion mutation (Figure 7) missing the C-terminus and N-terminus respectively show evidence of the importance of N-terminal end of ERD14 protein in its ability to shift in mass after phosphorylation by a kinase.

One of the characteristic features of CKII is its ability to phosphorylate ser/thr/tyr aa residues that are three residues upstream of an acidic residue (ser/thr-X-X-Glu/Asp).

ERD14 serines at position 83, 84 and 85 are each located three amino acid residues upstream of a glutamic acidic residue (Figure 6). Out of the three serines mentioned, serine at position 83 appears to be most important in phosphorylation and molecular mass shifting activities in ERD14. The serine at position 83 could be a crucial serine residue contributing heavily to activation of surrounding serines on the ERD14 S-region. This hypotheses is supported by evidence from the gel shift and $^{32}P$ incorporation results (Figure 12 & Figure 17) where mutations paired with serine at position 83 demonstrated a decrease in apparent mass shift efficiency and phosphate incorporation. Mutations at positions 84 and 85, when paired with a mutation at position 83, resulted in a decrease in mass shifting which was correlated with a decrease in $^{32}P$ incorporation compared to WT (GST-ERD14).

Furthermore, serines at position 83 and 85 together appear to be important for calcium binding activities related to phosphorylation by CKII. Gel shifting assay result (Figure 12) showed a decrease in apparent mass shifting capability of S83,85A mutant that correlated with a decrease in $^{32}P$ incorporation and loss of calcium binding activity (Figure 20) of the mutant. Calcium blot results from the truncated mutants (Figure 21) indicate the calcium binding region is localized between the S-region and the K-region near the C-terminal end. The model predicting calcium binding sites on ERD14 (Figure 26), indicates a possible calcium binding site that correlates with the observed results. The calcium binding site is predicted to be downstream of the S-region close to the serines at position 83, 84 and 85.

The triple mutant (S83,84,85A) loses all its ability to bind to calcium indicating these three positions together have a role to play in phosphorylation dependent calcium binding activities.

The substitution mutant D78N was created to compare phosphorylation and calcium binding behavior of ERD14 when it's S-region was mutated to one similar to ERD10 and COR47. Alsheikh et al., 2005 observed ERD10 and COR47 phosphorylation and calcium binding activities were less efficient than ERD14 (Figure 2). One of the key difference between ERD14 S-region and that of ERD10 and COR47 is the presence of aspartate (D78) residue on ERD14 whereas ERD10 and COR47 contain asparagine residue at the corresponding position (Figure 25). Mutation of aspartate to asparagine on ERD14 does not appear to have any effect on phosphorylation dependent calcium binding activities of ERD14. This implies that other sites in ERD10 and COR47 must be responsible for their decreased phosphorylation and calcium binding activities. Using the calcium binding site model (Appendix A5) of ERD14 to compare to ERD10 and COR47 protein sequences, both ERD10 and COR47 calcium binding site sequences appear to differ from ERD14 predicted calcium binding site sequence.

- ERD14

MAEEIKNVPEQEVPKVATEESSAEVTDRGLFDFLGKKKDETKPEETPIASEFEQKVHISEPEPEVKHE
SLLEKLHRSDSSSSSSSEEEGSDGEKRKKKKEKKKPTTEVEVKEEEKKGFMEKLKEKLPGHKKPEDGS
AVAAAPVVVPPPVEEAHPVEKKGILEKIKEKLPGYHPKTTVEEEKKDKE

- ERD10

MAEEYKNTVPEQETPKVATEESSAPEIKERGMFDFLKKKEEVKPQETTTLASEFEHKTQISEPESFVA
KHEEEEHKPTLLEQLHQKHEEEEENKPSLLDKLHRSNSSSSSSSDEEGEDGEKKKKEKKKKIVEGDH
VKTVEEENQGVMDRIKEKFPLGEKPGGDDVPVVTTMPAPHSVEDHKPEEEEKKGFMDKIKEKLP
GHSKKPEDSQVVNTTPLVETATPIADIPEEKKGFMDKIKEKLPGYHAKTTGEEEKKEKVSD

- COR47

MAEEYKNNVPEHETPTVATEESPATTTEVTDRGLFDFLGKKEEEVKPQETTTLESEFDHKAQISEPE
LAAEHEEVKENKITLLEELQEKTEEDEENKPSVIEKLHRSNSSSSSSSDEEGEEKKEKKKKIVEGEEDK
KGLVEKIKEKLPGHHDKTAEDDVPVSTTIPVPVSESVVEHDHPEEEKKGLVEKIKEKLPGHHDEKAE
DSPAVTSTPLVVTEHPVEPTTELPVEHPEEKKGILEKIKEKLPGYHAKTTEEEVKKEKESDD

Figure 24. Protein sequences for ERD14, ERD10 and COR47 showing their S-regions and their difference in the S-region. Underlined region is the S-region; Red star aa residue represent main difference between ERD14 and the other two dhns S-regions.

Purified truncated mutant T9.6 produced two unique bands on SDS-PAGE gel (~35 kD and ~51 kD) unlike the other two truncations (T3.5 and T6.2). The full sized band showed no apparent molecular mass shift (Figure 11) after being phosphorylated by CKII while the lower band did. However, both bands showed strong phosphate incorporation (Figure 14). In the calcium binding assay, only the lower band exhibited calcium binding activities (Figure 18). Identity of this lower band is unknown. It is possible the mutant construct has a proteolyzed product associated with it that has greater ability to incorporate phosphate and to bind calcium. Since all GST-ERD14 mutant constructs have been observed to run higher than their predicted mass on SDS-PAGE gels, the higher mass band (~51 kD) is hypothesized to be the T9.6 mutant (Appendix A1). Purified T9.6

is observed to run at ~51 kD contrary to the predicted ~44 kD mass (Appendix A1). Comparing calcium binding results for T3.5 and T6.2, one can deduce the location of the site most likely to play an important role in $Ca^{2+}$ binding. The model on figure 26 correlates with my observation that the $Ca^{2+}$ binding site is highly likely localized downstream and adjacent to the S-region.

The triple mutant (S83,84,85A) and truncated mutant (T6.2) compared to WT exhibit trace amounts of $^{32}P$ incorporation indicating there are sites other than the S-region that can be phosphorylated by CKII. Mass spectroscopy study carried out by Alsheikh et al., 2005 demonstrated there were other sites that could be phosphorylated by CKII (Appendix A4). However all the results shown here suggest these sites do not influence phosphorylation-dependent calcium binding activities of ERD14.

Another interesting observation was regarding the truncation mutant T9.6 which lacks the N-terminus (Figure 3). Purified T9.6 contained two bands uncharacteristic from all the other constructs (Figure 8). When phosphorylated by CKII, both bands showed $^{32}P$ incorporation (Figure 14) but the larger band exhibited no apparent shift in mass whereas the smaller band showed a shift in mass (Figure 11). Even further, the smaller band had calcium binding activity where the larger band showed no such activity. Currently it is unknown the exact identity of the two bands but the larger band could potentially contain an incomplete T9.6 sequence; a portion that contains the S-region necessary for CKII phosphorylation but lacks the remaining regions that are involved in apparent mass shifting and calcium binding activities.

After characterizing AtERD14 S-region *in vitro*, *in vivo* studies will help build an overall understanding of the relationship between phosphorylation-dependent calcium binding activity in the S-region and how it affects cold tolerance in Arabidopsis.

Dehydrins are predicted to be a redundant family. Ten Arabidopsis dehydrin genes have been characterized and they are observed to share similar sequences hinting at the possibility of overlapping functions of these genes (Puhakainen et al., 2004). Over expression of multiple dehydrin genes to freezing stress in Arabidopsis resulted in increased cold tolerance indicating the possibility of functional redundancy in the dehydrin family (Choi et al., 1999; Rodriguez et al., 2005). It is not surprising cold tolerance studies on single KO plants yielded no cold sensitive phenotype. The results indicate the need to KO multiple dehydrins in hopes of creating a phenotype. To carry out cold tolerance studies *in vivo*, T2 lines (144 samples) from T1 line selfing crosses were harvested but the genotypic PCR analysis necessary to locate a successful homozygous double KO event/s is not yet completed. The odds of a successful homozygous event is 1 out 16 in the 144 T2 lines.

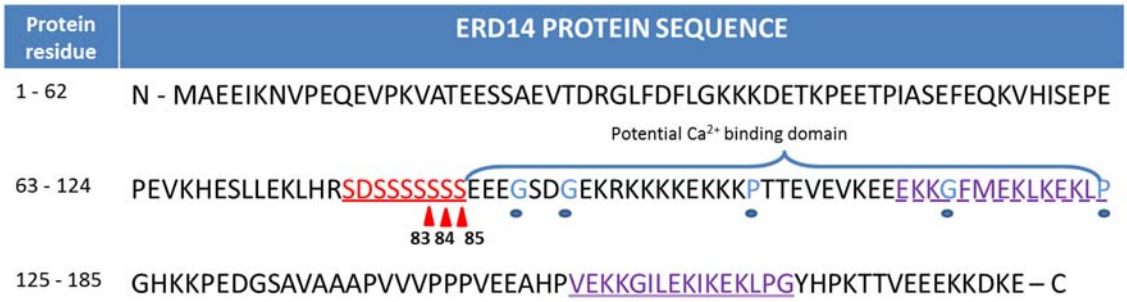


Figure 25. AtERD14 protein sequence summarizing areas that are crucial for phosphorylation-dependent calcium binding activities. S-region is single underlined and has red letters, K-region adjacent to the S-region has purple letters and is underlined with a dashed line; K-region near the C-terminus has purple letters and is double underlined with a wavy line. Possible calcium binding site is highlighted; dark blue letters indicate amino acids often involved in calcium-binding. Proline and glycines in putative calcium-binding domains are under-dotted (By Stephen Randall).

To summarize (Figure 26), the N-terminal end and the S-region of ERD14 are crucial sites for phosphorylation activities that regulate ERD14 structure and calcium binding activities. In the S-region specifically, the serine residue at position 83 is an important residue affecting ERD14 ability to properly incorporate phosphate in the S-region. Combined mutations at specific serine residues (S83,85A & S83,84,85A) in the S-region resulted in significant decrease in phosphorylation activity (Figure 14; Figure 15; Appendix A4) that correlated with the loss of ability for apparent shift in molecular mass (Figure 9 – Figure 11) and bind calcium (Figure 17). In light of the calcium binding assay results of the truncation mutants and the model predicting possible calcium binding sites on ERD14, the calcium binding site is predicted to be localized downstream of the S-region and adjacent to the S-region (Figure 16 & Figure 18). *In vivo* studies discovered

lack of cold tolerance phenotype from the single erd14, erd10 or cor47 KOs Arabidopsis plants prompting an attempt to create homozygous double KO transgenic plants. Understanding specific sites crucial for phosphorylation-dependent calcium binding activity can lead to further understanding of soybean dehydrins and how they can be engineered to confer cold tolerance in soybeans. This study will further assist in our understanding of roles of dehydrins during cold stress and our understanding of intrinsically disordered proteins.

# CHAPTER 5. PROSPECTUS

In this thesis, I discussed the important role the S-region and ERD14 N-terminal play in molecular mass shifting related to phosphorylation activities. From the results gleaned from these experiments, it is now possible to further characterize the N-terminal end to locate specific amino acid residues important for molecular mass shift in ERD14 via creation of a series of deletion mutations between the N-terminal end and the S-region. Also, it is possible for the S-region to have a direct or indirect interaction with the two AtERD14 K-regions since the K-regions are capable of forming A2 amphipathic α-helices providing secondary structure to the protein. It is feasible to carry out protein regional interaction studies to determine the S-region relationship with the two K-regions. Calcium binding region was discovered to localize in the region between the S-region and the K-region closest to the C-terminal end. To localize the region crucial for calcium binding activities, a series of deletion mutations will need to be created starting from the C-terminal end of the protein. According to the model predicting feasible calcium binding sites (Figure 26 & Appendix A4), one could be more precise and create mutations downstream and close to the S-region to characterize sites important for calcium binding on ERD14.

Another interesting study would be to create a single mutation at position 86, substituting glutamic acid for aspartic acid or creating the mutation in conjunction with a D78N mutation on ERD14 and observing the effect that has on phosphorylation and calcium binding activity in comparison to ERD10 and COR47 dehydrins.

As stated in the results, the purified truncated mutant T9.6 produced two bands (~35 kD and ~51 kD) uncharacteristic from the other constructs. To identify the two bands one can begin with probing the two bands with GST and ERD14 antibodies first to determine whether the bands have sequences of the two proteins. Another possibility is creating a construct missing the N-terminal and the C-terminal but containing all the conserved regions with the sequences in between to study this observation further. Furthermore, mass spectroscopy studies will need to be carried out to further characterize the two bands in order to understand the properties this particular truncation is exhibiting with regard to molecular mass shifting, phosphorylation and calcium binding activities.

Single KO transgenic lines failed to produce a cold sensitive phenotype, presumably due to functional redundancy in the acidic dehydrin family. To carry out cold tolerance studies *in vivo*, T2 (144 samples) from T1 line selfing were harvested but the genotyping necessary to identify a successful homozygous double KO event/s is not yet completed. After confirming a homozygous double KO event, the line/s can be used to determine whether or not the double KO event will develop a cold sensitive phenotype.

# REFERENCES

# REFERENCES

Agrawal, G. K., Agrawal, S. K., Shibato, J., Iwahashi, H., & Rakwal, R. (2003). "Novel rice MAP kinases involved in encountering diverse environmental stresses and developmental regulation." Biochemical and biophysical research communications 300(3): 775-783.

Alonso, Antonio, Cristina S. Queiroz, and Antonio C. Magalhães. "Chilling stress leads to increased cell membrane rigidity in roots of coffee (Coffea arabica L.) seedlings." *Biochimica et Biophysica Acta (BBA)-Biomembranes* 1323, no. 1 (1997): 75-84.

Alsheikh, M. K., B. J. Heyen, & Randall, S.K. (2003). "Ion binding properties of the dehydrin ERD14 are dependent upon phosphorylation." Journal of Biological Chemistry 278(42): 40882-40889.

Alsheikh, M. K., Svensson, J. T., & Randall, S. K. (2005). "Phosphorylation regulated ion-binding is a property shared by the acidic subclass dehydrins." Plant, Cell & Environment 28(9): 1114-1122.

Asghar, R., Fenton, R. D., DeMason, D. A., & Close, T. J. (1994). “Nuclear and cytoplasmic localization of maize embryo and aleurone dehydrin.” *Protoplasma*, *177*(3-4), 87-94.

Barclay, Katherine D., and Bryan D. McKersie. "Peroxidation reactions in plant membranes: effects of free fatty acids." *Lipids* 29, no. 12 (1994): 877-882.

Bokor, M., Csizmók, V., Kovács, D., Bánki, P., Friedrich, P., Tompa, P., & Tompa, K. (2005). “NMR relaxation studies on the hydrate layer of intrinsically unstructured proteins.” *Biophysical journal*, *88*(3), 2030-2037.

Borovskii, G. B., Stupnikova, I. V., Antipina, A. I., Downs, C. A., & Voinikov, V. K. (2000). “Accumulation of dehydrin-like-proteins in the mitochondria of cold-treated plants.” *Journal of plant physiology*, *156*(5), 797-800.

Bouche, N. and D. Bouchez (2001). "Arabidopsis gene knockout: phenotypes wanted." Current opinion in plant biology 4(2): 111-117.

Boyer, John S. "Plant productivity and environment." *Science* 218, no. 4571 (1982): 443-448.

Bray E.A, Bailey-Serres J, & Weretilnyk E (2000). “Responses to abiotic stresses.” Biochemistry and molecular biology of plants: 1158-1203.

Browse, J., & Xin, Z. (2001). “Temperature sensing and cold acclimation.” *Current opinion in plant biology*, *4*(3), 241-246.

Burke, M. J., Gusta, L. V., Quamme, H. A., Weiser, C. J., & Li, P. H. (1976). “Freezing and injury in plants.” *Annual Review of Plant Physiology*, *27*(1), 507-528.

Chen, C. P., & Walker, V. K. (1994). “Cold-shock and chilling tolerance in Drosophila.” *Journal of Insect Physiology*, *40*(8), 661-669.

Chew, Y. H. and K. J. Halliday (2011). "A stress-free walk from Arabidopsis to crops." Curr Opin Biotechnol 22(2): 281-286.

Chinnusamy, Viswanathan, Jianhua Zhu, and Jian-Kang Zhu. "Cold stress regulation of gene expression in plants." *Trends in plant science* 12, no. 10 (2007): 444-451.

Choi, D-W., B. Zhu, and T. J. Close. "The barley (Hordeum vulgare L.) dehydrin multigene family: sequences, allele types, chromosome assignments, and expression characteristics of 11 Dhn genes of cv Dicktoo." *Theoretical and Applied Genetics* 98, no. 8 (1999): 1234-1247.

Close, T. J. (1997). Dehydrins: a commonalty in the response of plants to dehydration and low temperature. *Physiologia Plantarum*, *100*(2), 291-296.

Conway, T., G. W. Sewell, and L. O. Ingram. "Glyceraldehyde-3-phosphate dehydrogenase gene from Zymomonas mobilis: cloning, sequencing, and identification of promoter region." *Journal of bacteriology* 169, no. 12 (1987): 5653-5662.

Danyluk, J., Houde, M., Rassart, É., & Sarhan, F. (1994). "Differential expression of a gene encoding an acidic dehydrin in chilling sensitive and freezing tolerant gramineae species." FEBS letters 344(1): 20-24.

Danyluk, Jean, André Perron, Mario Houde, Allen Limin, Brian Fowler, Nicole Benhamou, and Fathey Sarhan. "Accumulation of an acidic dehydrin in the vicinity of the plasma membrane during cold acclimation of wheat." *The Plant Cell Online* 10, no. 4 (1998): 623-638.

Davidson SW, Jonas A, Clayton DF, George JM *(*1998*) "Stabilization of alpha-synuclein secondary structure upon binding to synthetic membranes."* J Biol Chem 273**:** 9443–*9449.*

Davik, Jahn, Gage Koehler, Britta From, Torfinn Torp, Jens Rohloff, Petter Eidem, Robert C. Wilson, Anita Sønsteby, Stephen K. Randall, and Muath Alsheikh. "Dehydrin, alcohol dehydrogenase, and central metabolite levels are associated with cold tolerance in diploid strawberry (Fragaria spp.)." *Planta* 237, no. 1 (2013): 265-277.

Dunker, A. K., Brown, C. J., Lawson, J. D., Iakoucheva, L. M., & Obradovic, Z. (2002). Intrinsic disorder and protein function. *Biochemistry*, *41*(21), 6573-6582.

Dunker, A. K., Silman, I., Uversky, V. N., & Sussman, J. L. (2008). "Function and structure of inherently disordered proteins." *Current opinion in structural biology*, *18*(6), 756-764.

Dure III, L., Crouch, M., Harada, J., Ho, T. H. D., Mundy, J., Quatrano, R., & Sung, Z. R. (1989). "Common amino acid sequence domains among the LEA proteins of higher plants." *Plant Molecular Biology*, *12*(5), 475-486.

Eriksson, Sylvia K., and Pia Harryson. "Dehydrins: molecular biology, structure and function." In *Plant desiccation tolerance*, pp. 289-305. Springer Berlin Heidelberg, 2011.

Fink, Anthony L. "Natively unfolded proteins." *Current opinion in structural biology* 15, no. 1 (2005): 35-41.

Fowler, S., & Thomashow, M. F. (2002). "Arabidopsis transcriptome profiling indicates that multiple regulatory pathways are activated during cold acclimation in addition to the CBF cold response pathway." *The Plant Cell Online*, *14*(8), 1675-1690.

Frohnmeyer, Hanns, Linda Loyall, Michael R. Blatt, and Alexander Grabov. "Millisecond UV-B irradiation evokes prolonged elevation of cytosolic-free Ca2+ and stimulates gene expression in transgenic parsley cell cultures." *The Plant Journal* 20, no. 1 (1999): 109-117.

Gao, Dongjie, Marc R. Knight, Anthony J. Trewavas, Burkhard Sattelmacher, and Christoph Plieth. "Self-reporting Arabidopsis expressing pH and [Ca2+] indicators unveil ion dynamics in the cytoplasm and in the apoplast under abiotic stress." *Plant Physiology* 134, no. 3 (2004): 898-908.

Gilmour, Sarah J., Ravindra K. Hajela, and Michael F. Thomashow. "Cold acclimation in Arabidopsis thaliana." *Plant Physiology* 87, no. 3 (1988): 745-750.

Guy, C. L. (1990). “Cold accelimation and freezing stress tolerance: role of protein metabolism.” *Annual review of plant biology*, *41*(1), 187-223.

Hall, D. (2006). “Protein self-association in the cell: a mechanism for fine tuning the level of macromolecular crowding?” *European Biophysics Journal*, *35*(3), 276-280.

Hanin, M., Brini, F., Ebel, C., Toda, Y., Takeda, S., & Masmoudi, K. (2011). “Plant dehydrins and stress tolerance: versatile proteins for complex mechanisms.” *Plant signaling & behavior*, *6*(10), 1503.

Hara, M., Fujinaga, M., & Kuboi, T. (2004). “Radical scavenging activity and oxidative modification of citrus dehydrin.” *Plant Physiology and Biochemistry*, *42*(7), 657-662.

Hara, M., Fujinaga, M., & Kuboi, T. (2005). “Metal binding by citrus dehydrin with histidine-rich domains.” *Journal of experimental botany*, *56*(420), 2695-2703.

Hara, M., Terashima, S., & Kuboi, T. (2001). “Characterization and cryoprotective activity of cold-responsive dehydrin from Citrus unshiu.” *Journal of Plant Physiology*, *158*(10), 1333-1339.

Hara, M., Terashima, S., Fukaya, T., & Kuboi, T. (2003). “Enhancement of cold tolerance and inhibition of lipid peroxidation by citrus dehydrin in transgenic tobacco.” *Planta*, *217*(2), 290-298.

Heino, P., & Palva, E. T. (2004). Signal transduction in plant cold acclimation. In *Plant Responses to Abiotic Stress* (pp. 151-186). Springer Berlin Heidelberg.

Hellergren, J., Widell, S., Lundborg, T., & Kylin, A. (1983). “Frosthardiness development in Pinus sylvestris: The involvement of a K+-stimulated Mg2+-dependent ATPase from purified plasma membranes of pine.” *Physiologia Plantarum*, *58*(1), 7-12.

Heyen, B. J., Alsheikh, M. K., Smith, E. A., Torvik, C. F., Seals, D. F., & Randall, S. K. (2002). "The calcium-binding activity of a vacuole-associated, dehydrin-like protein is regulated by phosphorylation." Plant Physiology 130(2): 675-687.

Hoekstra, Folkert A., Elena A. Golovina, and Julia Buitink. "Mechanisms of plant desiccation tolerance." *Trends in plant science* 6, no. 9 (2001): 431-438.

Horvath, Ibolya, Attila Glatz, Viktória Varvasovszki, Zsolt Török, Tibor Páli, Gábor Balogh, Eszter Kovács et al. "Membrane physical state controls the signaling mechanism of the heat shock response in Synechocystis PCC 6803: identification of hsp17 as a “fluidity gene”." *Proceedings of the National Academy of Sciences* 95, no. 7 (1998): 3513-3518.

Houde, M., Dallaire, S., N'Dong, D., & Sarhan, F. (2004). "Overexpression of the acidic dehydrin WCOR410 improves freezing tolerance in transgenic strawberry leaves." Plant Biotechnology Journal 2(5): 381-387.

Houde, Mario, Jean Danyluk, Jean-François Laliberté, Eric Rassart, Rajinder S. Dhindsa, and Fathey Sarhan. "Cloning, characterization, and expression of a cDNA encoding a 50-kilodalton protein specifically induced by cold acclimation in wheat." *Plant physiology* 99, no. 4 (1992): 1381-1387.

Hume, D. J., and Ann KH Jackson. "Pod formation in soybeans at low temperatures." *Crop Science* 21, no. 6 (1981): 933-937.

Hundertmark, M. and D. K. Hincha (2008). "LEA (late embryogenesis abundant) proteins and their encoding genes in Arabidopsis thaliana." BMC genomics 9(1): 118.

Ibrahim el SM, Rahman AK, Isoda R, Umeda K, Van Sa N, Kodama Y (2008). "*In vitro* and in vivo effectiveness of egg yolk antibody against Candida albicans (anti-CA IgY)." Vaccine 26: 2073-2080

Ingram, J. and D. Bartels (1996). "The molecular basis of dehydration tolerance in plants." Annual review of plant biology 47(1): 377-403.

Ismail, A. M., Hall, A. E., & Close, T. J. (1999). "Purification and partial characterization of a dehydrin involved in chilling tolerance during seedling emergence of cowpea." Plant Physiology 120(1): 237-244.

Jan, N., & Andrabi, K. I. (2009). "Cold resistance in plants: A mystery unresolved." *Electronic Journal of Biotechnology*, *12*(3), 14-15.

Kacperska, A. (1989). "Metabolic consequences of low temperature stress in chilling-insensitive plants."

Kazuoka, T., & Oeda, K. (1994). Purification and characterization of COR85-oligomeric complex from cold-acclimated spinach. *Plant and cell physiology*, *35*(4), 601-611.

Kenefick, D. G., and C. R. Swanson. "Mitochondrial activity in cold acclimated winter barley." *Crop Science* 3, no. 3 (1963): 202-205.

Kim, K. N., Cheong, Y. H., Grant, J. J., Pandey, G. K., & Luan, S. (2003). "CIPK3, a calcium sensor–associated protein kinase that regulates abscisic acid and cold signal transduction in Arabidopsis." The Plant Cell Online 15(2): 411-423.

Kim, K. N., Cheong, Y. H., Gupta, R., & Luan, S. (2000). "Interaction specificity of Arabidopsis calcineurin B-like calcium sensors and their target kinases." Plant Physiology 124(4): 1844-1853.

Kiyosue, T., Yamaguchi-Shinozaki, K., & Shinozaki, K. (1994). "Characterization of two cDNAs (ERD10 and ERD14) corresponding to genes that respond rapidly to dehydration stress in Arabidopsis thaliana." Plant and Cell Physiology 35(2): 225-231.

Knight, H., Trewavas, A. J., & Knight, M. R. (1996). "Cold calcium signaling in Arabidopsis involves two cellular pools and a change in calcium signature after acclimation." The Plant Cell Online 8(3): 489-503.

Knight, Heather, and Marc R. Knight. "Imaging spatial and cellular characteristics of low temperature calcium signature after cold acclimation in Arabidopsis." *Journal of experimental botany* 51, no. 351 (2000): 1679-1686.

Knight, M. R. (2002). "Signal transduction leading to low–temperature tolerance in Arabidopsis thaliana." Philosophical Transactions of the Royal Society of London. Series B: Biological Sciences 357(1423): 871-875.

Knight, M. R., Campbell, A. K., Smith, S. M., & Trewavas, A. J. (1991). “Transgenic plant aequorin reports the effects of touch and cold-shock and elicitors on cytoplasmic calcium.”

Knight, Marc R., and Heather Knight. "Low-temperature perception leading to gene expression and cold tolerance in higher plants." *New Phytologist* 195, no. 4 (2012): 737-751.

Koag, M. C., Wilkens, S., Fenton, R. D., Resnik, J., Vo, E., & Close, T. J. (2009). “The K-segment of maize DHN1 mediates binding to anionic phospholipid vesicles and concomitant structural changes.” *Plant physiology*, *150*(3), 1503-1514.

Koag, Myong-Chul, Raymond D. Fenton, Stephan Wilkens, and Timothy J. Close. "The binding of maize DHN1 to lipid vesicles. Gain of structure and lipid specificity." *Plant Physiology* 131, no. 1 (2003): 309-316.

Kodama, Hiroaki, Tatsurou Hamada, Gorou Horiguchi, Mitsuo Nishimura, and Koh Iba. "Genetic enhancement of cold tolerance by expression of a gene for chloroplast [omega]-3 fatty acid desaturase in transgenic tobacco." *Plant Physiology* 105, no. 2 (1994): 601-605.

Koehler Gage, W. T. J., Randall Stephen (2007). "Transcript expression analysis indicates distinct roles for dehydrin subclasses." Current topics in phytochemistry 8: 73-83.

Kosova, K., Vítámvás, P., & Prášil, I. T. (2007). "The role of dehydrins in plant response to cold." Biologia Plantarum 51(4): 601-617.

Kovacs, D., Kalmar, E., Torok, Z., & Tompa, P. (2008). "Chaperone activity of ERD10 and ERD14, two disordered stress-related plant proteins." Plant Physiology 147(1): 381-390.

Kramerov, A. A. and A. V. Ljubimov (2012). "Focus on Molecules: Protein kinase CK2." Experimental eye research 101: 111.

Kreps, J. A., Wu, Y., Chang, H. S., Zhu, T., Wang, X., & Harper, J. F. (2002). "Transcriptome changes for Arabidopsis in response to salt, osmotic, and cold stress." *Plant Physiology*, *130*(4), 2129-2141.

Kruger, C., Berkowitz, O., Stephan, U. W., & Hell, R. (2002). "A Metal-binding Member of the Late Embryogenesis Abundant Protein Family Transports Iron in the Phloem of Ricinus communis L." *Journal of Biological Chemistry*, *277*(28), 25062-25069.

Lang, V., Heino, P., & Palva, E. T. (1989). "Low temperature acclimation and treatment with exogenous abscisic acid induce common polypeptides in *Arabidopsis thaliana* (L.) Heynh." *Theoretical and applied genetics*, *77*(5), 729-734.

Lee, S. P., Zhu, B., Chen, T. H., & Li, P. H. (1992). "Induction of freezing tolerance in potato (Solanum commersonü) suspension cultured cells." *Physiologia Plantarum*, *84*(1), 41-48.

Levitt, J. (1980). "*Responses of plants to environmental stresses. Volume II. Water, radiation, salt, and other stresses* (No. Ed. 2)." Academic Press.

Lewis, Bryan D., George Karlin-Neumann, Ronald W. Davis, and Edgar P. Spalding. "Ca2+-activated anion channels and membrane depolarizations induced by blue light and cold in Arabidopsis seedlings." *Plant physiology* 114, no. 4 (1997): 1327-1334.

Lisse, T., Bartels, D., Kalbitzer, H. R., & Jaenicke, R. (1996). "The recombinant dehydrin-like desiccation stress protein from the resurrection plant Craterostigma plantagineum displays no defined three-dimensional structure in its native state." *Biological chemistry*, *377*(9), 555-562.

Lopez, C. G., Banowetz, G. M., Peterson, C. J., & Kronstad, W. E. (2003). "Dehydrin expression and drought tolerance in seven wheat cultivars." *Crop Science*, *43*(2), 577-582.

Luo, P., & Baldwin, R. L. (1997). “Mechanism of helix induction by trifluoroethanol: a framework for extrapolating the helix-forming properties of peptides from trifluoroethanol/water mixtures back to water.” *Biochemistry*, *36*(27), 8413-8421.

Mahajan, S., & Tuteja, N. (2005). “Cold, salinity and drought stresses: an overview.” *Archives of biochemistry and biophysics*, *444*(2), 139-158.

Martiniere, A., Shvedunova, M., Thomson, A. J., Evans, N. H., Penfield, S., Runions, J., & McWatters, H. G. (2011). “Homeostasis of plasma membrane viscosity in fluctuating temperatures.” *New Phytologist*, *192*(2), 328-337.

Maximov, N. A. (1929). “Internal factors of frost and drought resistance in plants.” *Protoplasma*, *7*(1), 259-291.

McNulty, B. C., Tripathy, A., Young, G. B., Charlton, L. M., Orans, J., & Pielak, G. J. (2006). “Temperature-induced reversible conformational change in the first 100 residues of α-synuclein.” *Protein science*, *15*(3), 602-608.

Medina, J., Bargues, M., Terol, J., Pérez-Alonso, M., & Salinas, J. (1999). "The Arabidopsis CBF gene family is composed of three genes encoding AP2 domain-containing proteins whose expression is regulated by low temperature but not by abscisic acid or dehydration." Plant Physiology 119(2): 463-470.

Meggio, F., & PINNA, L. A. (2003). “One-thousand-and-one substrates of protein kinase CK2?” The FASEB Journal, 17(3), 349-368.

Minton, A. P. (2005a). “Influence of macromolecular crowding upon the stability and state of association of proteins: predictions and observations.” *Journal of pharmaceutical sciences*, *94*(8), 1668-1675.

Mithofer, Axel, and Christian Mazars. "Aequorin-based measurements of intracellular Ca2+-signatures in plant cells." Biological procedures online 4, no. 1 (2002): 105-118.

Miura, K. and T. Furumoto (2013). "Cold Signaling and Cold Response in Plants." International Journal of Molecular Sciences 14(3): 5312-5337.

Mohapatra, S. S., Poole, R. J., & Dhindsa, R. S. (1987). “Changes in protein patterns and translatable messenger RNA populations during cold acclimation of alfalfa.” *Plant physiology*, *84*(4), 1172-1176.

Monroy, A. F., & Dhindsa, R. S. (1995). “Low-temperature signal transduction: induction of cold acclimation-specific genes of alfalfa by calcium at 25 degrees C.” *The Plant Cell Online*, *7*(3), 321-331.

Mouillon, J. M., Gustafsson, P., & Harryson, P. (2006). "Structural investigation of disordered stress proteins. Comparison of full-length dehydrins with isolated peptides of their conserved segments." Plant Physiology 141(2): 638-650.

Murata, N., P. S. Mohanty, H. Hayashi, and G. C. Papageorgiou. "Glycinebetaine stabilizes the association of extrinsic proteins with the photosynthetic oxygen-evolving complex." *FEBS letters* 296, no. 2 (1992): 187-189.

Narusaka, Yoshihiro, Kazuo Nakashima, Zabta K. Shinwari, Yoh Sakuma, Takashi Furihata, Hiroshi Abe, Mari Narusaka, Kazuo Shinozaki, and Kazuko Yamaguchi-Shinozaki. "Interaction between two cis-acting elements, ABRE and DRE, in ABA-dependent expression of Arabidopsis rd29A gene in response to dehydration and high-salinity stresses." *The Plant Journal* 34, no. 2 (2003): 137-148.

Nylander, M., Svensson, J., Palva, E. T., & Welin, B. V. (2001). “Stress-induced accumulation and tissue-specific localization of dehydrins in Arabidopsis thaliana.” *Plant molecular biology*, *45*(3), 263-279.

O’Brien, J. A., Daudi, A., Butt, V. S., & Bolwell, G. P. (2012). “Reactive oxygen species and their role in plant defence and cell wall metabolism.” *Planta*, *236*(3), 765-779.

Ochoa-Alfaro, A. E., Rodríguez-Kessler, M., Pérez-Morales, M. B., Delgado-Sánchez, P., Cuevas-Velazquez, C. L., Gómez-Anduro, G., & Jiménez-Bremont, J. F. (2012). "Functional characterization of an acidic SK3 dehydrin isolated from an *Opuntia streptacantha* cDNA library." Planta 235(3): 565-578.

Orvar BL, Sangwan V, Omann F & Dhindsa RS (2000). “Early steps in cold sensing by plant cells: the role of actin cytoskeleton and membrane fluidity.” The Plant Journal 23(6):785-794.

Palta, J. P. (1989). “Plasma membrane ATPase as a key site of perturbation in response to freeze-thaw stress.” In *Current topics in plant biochemistry and physiology: Proceedings of the... Plant Biochemistry and Physiology Symposium held at the University of Missouri, Columbia (USA)*.

Pearce, S. R., Stuart-Rogers, C., Knox, M. R., Kumar, A., Ellis, T. H., & Flavell, A. J. (1999). “Rapid isolation of plant Ty1-copia group retrotransposon LTR sequences for molecular marker studies.” *The Plant Journal*, *19*(6), 711-717.

Peng, Y., Lin, W., Cai, W., & Arora, R. (2007). "Overexpression of a Panax ginseng tonoplast aquaporin alters salt tolerance, drought tolerance and cold acclimation ability in transgenic Arabidopsis plants." Planta 226(3): 729-740.

Percival, Glynn C., Celia Boyle, and Lynn Baird. "The influence of calcium supplementation on the freezing tolerance of woody plants." *Journal of Arboriculture* 25 (1999): 285-291.

Plana, Maria, E. Itarte, R. Eritja, A. Goday, M. Pages, and M. Carmen Martínez. "Phosphorylation of maize RAB-17 protein by casein kinase 2." *Journal of Biological Chemistry* 266, no. 33 (1991): 22510-22514.

Polisensky, D. H. and J. Braam (1996). "Cold-shock regulation of the Arabidopsis TCH genes and the effects of modulating intracellular calcium levels." Plant Physiology 111(4): 1271-1279.

Puhakainen, T., Hess, M. W., Mäkelä, P., Svensson, J., Heino, P., & Palva, E. T. (2004). "Overexpression of multiple dehydrin genes enhances tolerance to freezing stress in Arabidopsis." *Plant molecular biology*, *54*(5), 743-753.

Qin, Feng, Kazuo Shinozaki, and Kazuko Yamaguchi-Shinozaki. "Achievements and challenges in understanding plant abiotic stress responses and tolerance." *Plant and Cell Physiology* 52, no. 9 (2011): 1569-1582.

Ramankutty, N., Evan, A. T., Monfreda, C., & Foley, J. A. (2008). "Farming the planet: 1. Geographic distribution of global agricultural lands in the year 2000." Global Biogeochemical Cycles 22(1).

Romeis, T., Ludwig, A. A., Martin, R., & Jones, J. D. (2001). "Calcium-dependent protein kinases play an essential role in a plant defense response." The EMBO journal 20(20): 5556-5567.

Rorat, T., Grygorowicz, W. J., Irzykowski, W., & Rey, P. (2004). "Expression of KS-type dehydrins is primarily regulated by factors related to organ type and leaf developmental stage during vegetative growth." *Planta*, *218*(5), 878-885.

Rorat, T., Szabala, B. M., Grygorowicz, W. J., Wojtowicz, B., Yin, Z., & Rey, P. (2006). "Expression of SK3-type dehydrin in transporting organs is associated with cold acclimation in Solanum species." *Planta*, *224*(1), 205-221.

Roux, S. J., and R. D. Slocum. "Role of calcium in mediating cellular functions important for growth and development in higher plants." *Calcium and cell function* 3 (1982): 409-453.

Rudrabhatla, P. and R. Rajasekharan (2002). "Developmentally regulated dual-specificity kinase from peanut that is induced by abiotic stresses." Plant Physiology 130(1): 380-390.

Sanders, D., Brownlee, C., & Harper, J. F. (1999). "Communicating with calcium." The Plant Cell Online 11(4): 691-706.

Sangwan, V., Foulds, I., Singh, J., & Dhindsa, R. S. (2001). “Cold-activation of Brassica napus BN115 promoter is mediated by structural changes in membranes and cytoskeleton, and requires Ca2+ influx.” *The Plant Journal*, *27*(1), 1-12.

Sangwan, Veena, Björn Lárus Örvar, John Beyerly, Heribert Hirt, and Rajinder S. Dhindsa. "Opposite changes in membrane fluidity mimic cold and heat stress activation of distinct plant MAP kinase pathways." *The Plant Journal* 31, no. 5 (2002): 629-638.

Sankaram, Mantripragada B., and Derek Marsh. "Protein-lipid interactions with peripheral membrane proteins." *New comprehensive biochemistry* 25 (1993): 127-162.

Segrest, J. P., De Loof, H., Dohlman, J. G., Brouillette, C. G., & Anantharamaiah, G. M. (1990). “Amphipathic helix motif: classes and properties.” Proteins: Structure, Function, and Bioinformatics, *8*(2), 103-117.

Seki, M., Narusaka, M., Abe, H., Kasuga, M., Yamaguchi-Shinozaki, K., Carninci, P., & Shinozaki, K. (2001). “Monitoring the expression pattern of 1300 Arabidopsis genes under drought and cold stresses by using a full-length cDNA microarray.” *The Plant Cell Online*, *13*(1), 61-72.

Seki, M., Narusaka, M., Ishida, J., Nanjo, T., Fujita, M., Oono, Y. & Shinozaki, K. (2002). “Monitoring the expression profiles of 7000 Arabidopsis genes under drought, cold and high-salinity stresses using a full-length cDNA microarray.” *The Plant Journal*, *31*(3), 279-292.

Sharma, P., Sharma, N., & Deswal, R. (2005). “The molecular biology of the low-temperature response in plants.” *Bioessays*, *27*(10), 1048-1059.

Shen, Y., Tang, M. J., Hu, Y. L., & Lin, Z. P. (2004). "Isolation and characterization of a dehydrin-like gene from drought-tolerant Boea crassifolia." Plant Science 166(5): 1167-1175.

Shinozaki, K. and K. Yamaguchi-Shinozaki (1997). "Gene expression and signal transduction in water-stress response." Plant Physiology 115(2): 327.

Shinozaki, K., Yamaguchi-Shinozaki, K., & Seki, M. (2003). “Regulatory network of gene expression in the drought and cold stress responses.” *Current opinion in plant biology*, *6*(5), 410-417.

Sigal, C. T., Zhou, W., Buser, C. A., McLaughlin, S., & Resh, M. D. (1994). "Amino-terminal basic residues of Src mediate membrane binding through electrostatic interaction with acidic phospholipids." Proceedings of the National Academy of Sciences 91(25): 12253-12257.

Smallwood, Maggie, and Dianna J. Bowles. "Plants in a cold climate." *Philosophical Transactions of the Royal Society of London. Series B: Biological Sciences* 357, no. 1423 (2002): 831-847.

Soulages, J. L., Kim, K., Arrese, E. L., Walters, C., & Cushman, J. C. (2003). "Conformation of a group 2 late embryogenesis abundant protein from soybean. Evidence of poly (L-proline)-type II structure." *Plant Physiology*, *131*(3), 963-975.

Steponkus, P. L. (1984). "Role of the plasma membrane in freezing injury and cold acclimation." *Annual Review of Plant Physiology*, *35*(1), 543-584.

Steponkus, P. L., & Lynch, D. V. (1989). "Freeze/thaw-induced destabilization of the plasma membrane and the effects of cold acclimation." *Journal of bioenergetics and biomembranes*, *21*(1), 21-41.

Steponkus, P. L., & Webb, M. S. (1992). "Freeze-induced dehydration and membrane destabilization in plants." In *Water and Life* (pp. 338-362). Springer Berlin Heidelberg.

Steponkus, P. L., D. V. Lynch, M. Uemura, U. Heber, and R. S. Pearce. "The Influence of Cold Acclimation on the Lipid Composition and Cryobehaviour of the Plasma Membrane of Isolated Rye Protoplasts [and Discussion]." *Philosophical Transactions of the Royal Society of London. B, Biological Sciences* 326, no. 1237 (1990): 571-583.

Steponkus, P. L., Uemura, M., & Webb, M. S. (1993). "A contrast of the cryostability of the plasma membrane of winter rye and spring oat-two species that widely differ in their freezing tolerance and plasma membrane lipid composition." *Advances in low-temperature biology*, *2*, 211-312.

Sterky, Fredrik, Rupali R. Bhalerao, Per Unneberg, Bo Segerman, Peter Nilsson, Amy M. Brunner, Laurence Charbonnel-Campaa et al. "A Populus EST resource for plant functional genomics." *Proceedings of the National Academy of Sciences of the United States of America* 101, no. 38 (2004): 13951-13956.

Sutinen, M. L., Palta, J. P., & Reich, P. B. (1992). "Seasonal differences in freezing stress resistance of needles of Pinus nigra and Pinus resinosa: evaluation of the electrolyte leakage method." *Tree Physiology*, *11*(3), 241-254.

Svensson, J., Palva, E. T., & Welin, B. (2000). "Purification of Recombinant Arabidopsis thaliana Dehydrins by Metal Ion Affinity Chromatography." Protein expression and purification 20(2): 169-178.

Teige, Markus, Elisabeth Scheikl, Thomas Eulgem, Róbert Dóczi, Kazuya Ichimura, Kazuo Shinozaki, Jeffery L. Dangl, and Heribert Hirt. "The MKK2 Pathway Mediates Cold and Salt Stress Signaling in Arabidopsis." *Molecular cell* 15, no. 1 (2004): 141-152.

Thomashow, M. F. (1998). "Role of cold-responsive genes in plant freezing tolerance." Plant Physiology 118(1): 1-8.

Thomashow, M. F. (1999). "Plant cold acclimation: freezing tolerance genes and regulatory mechanisms." Annual review of plant biology 50(1): 571-599.

Thomashow, M. F., Gilmour, S. J., Stockinger, E. J., Jaglo-Ottosen, K. R., & Zarka, D. G. (2001). “Role of the Arabidopsis CBF transcriptional activators in cold acclimation.” *Physiologia Plantarum*, *112*(2), 171-175.

Tissier, Alain F., Sylvestre Marillonnet, Victor Klimyuk, Kanu Patel, Miguel Angel Torres, George Murphy, and Jonathan DG Jones. "Multiple independent defective suppressor-mutator transposon insertions in Arabidopsis: a tool for functional genomics." *The Plant Cell Online* 11, no. 10 (1999): 1841-1852.

Tornroth-Horsefield, Susanna, Yi Wang, Kristina Hedfalk, Urban Johanson, Maria Karlsson, Emad Tajkhorshid, Richard Neutze, and Per Kjellbom. "Structural mechanism of plant aquaporin gating." *Nature* 439, no. 7077 (2006): 688-694.

Trewavas, Anthony. "Le calcium, c'est la vie: calcium makes waves." *Plant Physiology* 120, no. 1 (1999): 1-6.

Uemura, M., Joseph, R. A., & Steponkus, P. L. (1995). “Cold acclimation of Arabidopsis thaliana (effect on plasma membrane lipid composition and freeze-induced lesions).” *Plant physiology*, *109*(1), 15-30.

Uemura, M., Tominaga, Y., Nakagawara, C., Shigematsu, S., Minami, A., & Kawamura, Y. (2006). "Responses of the plasma membrane to low temperatures." Physiologia Plantarum 126(1): 81-89.

Uversky, V. N., Oldfield, C. J., & Dunker, A. K. (2005). “Showing your ID: intrinsic disorder as an ID for recognition, regulation and cell signaling.” *Journal of Molecular Recognition*, *18*(5), 343-384.

Van Buskirk, H. A., & Thomashow, M. F. (2006). “Arabidopsis transcription factors regulating cold acclimation.” *Physiologia Plantarum*, *126*(1), 72-80.

Van der Luit, A. H., Olivari, C., Haley, A., Knight, M. R., & Trewavas, A. J. (1999). "Distinct calcium signaling pathways regulate calmodulin gene expression in tobacco." Plant Physiology 121(3): 705-714.

Vazquez-Tello, A., Ouellet, F., & Sarhan, F. (1998). "Low temperature-stimulated phosphorylation regulates the binding of nuclear factors to the promoter of Wcs120, a cold-specific gene in wheat." Molecular and General Genetics MGG 257(2): 157-166.

Vogel, J. T., Zarka, D. G., Van Buskirk, H. A., Fowler, S. G., & Thomashow, M. F. (2005). “Roles of the CBF2 and ZAT12 transcription factors in configuring the low temperature transcriptome of Arabidopsis.” *The Plant Journal*, *41*(2), 195-211.

Wang W, Vinocur B, Shoseyov O, & Altman A (2000). “Biotechnology of plant osmotic stress tolerance physiological and molecular considerations.” IV International Symposium on *In Vitro* Culture and Horticultural Breeding 560, pp 285-292.

Wasteneys, G. O., & Galway, M. E. (2003). “Remodeling the cytoskeleton for growth and form: an overview with some new views.” *Annual Review of Plant Biology*, *54*(1), 691-722.

Waterhouse, P. M. and C. A. Helliwell (2003). "Exploring plant genomes by RNA-induced gene silencing." Nature Reviews Genetics 4(1): 29-38.

Webb, M. S., & Steponkus, P. L. (1993). “Freeze-induced membrane ultrastructural alterations in rye (Secale cereale) leaves.” *Plant physiology*, *101*(3), 955-963.

Webb, M. S., Uemura, M., & Steponkus, P. L. (1994). “A comparison of freezing injury in oat and rye: two cereals at the extremes of freezing tolerance.” *Plant physiology*, *104*(2), 467-478.

Wisniewski, M., Webb, R., Balsamo, R., Close, T. J., Yu, X. M., & Griffith, M. (1999). “Purification, immunolocalization, cryoprotective, and antifreeze activity of PCA60: a dehydrin from peach (Prunus persica).” *Physiologia Plantarum*, *105*(4), 600-608.

Wright, Peter E., and H. Jane Dyson. "Linking folding and binding." *Current opinion in structural biology* 19, no. 1 (2009): 31-38.

Xiong, Liming, Karen S. Schumaker, and Jian-Kang Zhu. "Cell signaling during cold, drought, and salt stress." *The Plant Cell Online* 14, no. suppl 1 (2002): S165-S183.

Xu, Q., Fu, H. H., Gupta, R., & Luan, S. (1998). "Molecular characterization of a tyrosine-specific protein phosphatase encoded by a stress-responsive gene in Arabidopsis." The Plant Cell Online 10(5): 849-857.

Yamaguchi-Shinozaki, K. and K. Shinozaki (1994). "A novel cis-acting element in an Arabidopsis gene is involved in responsiveness to drought, low-temperature, or high-salt stress." The Plant Cell Online 6(2): 251-264.

Zhu, B., Choi, D. W., Fenton, R., & Close, T. J. (2000). “Expression of the barley dehydrin multigene family and the development of freezing tolerance.” *Molecular and General Genetics MGG*, *264*(1-2), 145-153.

# APPENDIX

# APPENDIX

Appendix 1. Predicted molecular weight (MW) vs measured/observed molecular weight (MW). Measured MW was within 20% of the predicted MW.

| Sample ID | Clones | Predicted MW | Observed MW | PI |
|---|---|---|---|---|
| | ERD14 | 20.8 | | 5.41 |
| AC1 | S83,84,85A | 52.4 | 67.9 | 5.71 |
| AC2 | S83,85A | 52.4 | 67.9 | 5.71 |
| AC3 | S83,84A | 52.4 | 66.5 | 5.71 |
| AC4 | S84,85A | 52.4 | 66.5 | 5.71 |
| AC5 | S83A | 52.4 | 65.3 | 5.71 |
| AC6 | S85A | 52.4 | 65.3 | 5.71 |
| AC7 | S77A | 52.4 | 65.3 | 5.71 |
| AC8 | S79A | 52.4 | 63.9 | 5.71 |
| AC9 | D78N | 52.4 | 63.9 | 5.77 |
| AC10 | T3 | 46.3 | 44.6 | 5.56 |

Appendix 1 Continued

| | | | | |
|---|---|---|---|---|
| AC11 | T3.5 | 46.3 | 57.6 | 5.56 |
| AC12 | T6.2 | 42.3 | 53.5 | 5.50 |
| AC13 | S84A | 52.4 | 63.9 | 5.71 |
| AC14 | GST-ERD14 | 52.4 | 63.9 | 5.71 |
| AC15 | GST | 35.7 | 34.0 | 6.23 |
| AC16 | T9.6 | 43.7 | 51.5 | 6.18 |

MSPILGYWKIKGLVQPTRLLLEYLEEKYEEHLYERDEGDKWRNKKFELGLEFPNLPYYIDGDVKLTQSMAIIRYIADKHNM
LGGCPKERAEISMLEGAVLDIRYGVSRIAYSKDFETLKVDFLSKLPEMLKMFEDRLCHKTYLNGDHVTHPDFMLYDALDV
VLYMDPMCLDAFPKLVCFKKRIEAIPQIDKYLKSSKYIAWPLQGWQATFGGGDHPPKSDGSTSGSGHHHHHHSAGLVP
RGSTAIGMKETAAAKFERQHMDSPDLGTGGGSGDDDDKSPMAEEIKNVPEQEVPKVATEESSAEVTDRGLFDFLGKK
KDETKPEETPIASEFEQKVHISEPEPEVKHESLLEKLHFSDSSSSSSSEEEGSDGEKRKKKKEKKKPTTEVEVKEEEKKGFME
KLKEKLPGHKKPEDGSAVAAAPVVVPPPVEEAHPVEKKGILEKIKEKLPGYHPKTTVEEEKKDKE

Appendix 2. Full GST-ERD14 fusion protein sequence. Grey highlight represents GST protein sequence. Blue font highlight sequence represent linker sequence. Yellow highlight represents ERD14 protein sequence.

Appendix 3. T-test results for averaged $^{32}P$ incorporation into GST-ERD14 mutants at 5 minutes (n = 4) normalized to WT exhibiting significance relationship (5% P-value). $^{32}P$ incorporated values were divided by the protein values for each experiment before averaging the values.

| Mutant ID | WT vs | S77A vs | D78N vs | S83A vs | S84A vs | S85A vs | S83,84,85A vs | GST vs | T3.5 vs |
|---|---|---|---|---|---|---|---|---|---|
| S77A | 0.2143 | | | | | | | | |
| D78N | 0.9598 | | | | | | | | |
| S83A | 0.0411 | | | | | | | | |
| S84A | 0.9579 | | | | | | | | |
| S85A | 0.7828 | | | | | | | | |
| S83,84A | 0.0329 | 0.0407 | 0.0366 | 0.1787 | 0.1919 | 0.1393 | 0.1059 | | |
| S83,85A | 0.0019 | 0.0171 | 0.0027 | 0.0201 | 0.0862 | 0.0636 | 0.1306 | | |
| S84,85A | 0.7394 | 0.3313 | 0.7448 | 0.8270 | 0.8108 | 0.6680 | 0.1311 | | |
| S83,84,85A | 0.00001 | | | 0.0014 | 0.0384 | 0.0296 | | 0.3302 | |
| T3.5 | 0.1609 | | | | | | | | |
| T6.2 | 0.00001 | | | | | | | 0.2847 | 0.0264 |
| T9.6 | 0.2053 | | | | | | | | 0.9897 |

| Peptide Position(Peptide No.) | Peptide Sequence | Phosphorylation time (min) | No. of phosphorylation sites 1 | 2 | 3 |
|---|---|---|---|---|---|
| | ***In vitro phosphorylated ERD14*** | | | | |
| 16-28(I) | VATEESSAVTDR | 0 | - | - | - |
| | | 30 | - | - | - |
| | | 180 | b | - | - |
| 43-55(II) | PEETPISEFEQK | 0 | - | - | - |
| | | 30 | a, b | - | - |
| | | 180 | b | - | - |
| 56-66(III) | VHISEPEPEVK | 0 | - | - | - |
| | | 30 | a, b | - | - |
| | | 180 | b | - | - |
| 77-94(IV) | SDSSSSSSSEEEGSDGEK | 0 | - | - | - |
| | | 30 | a, b, c | c | - |
| | | 180 | a, b, c | a, b, c | a, b |
| 104-111(V) | PTTEVEVK | 0 | - | - | - |
| | | 30 | c | - | - |
| | | 180 | c, b | c, b | - |
| 175-181(VII) | TTVEEEK | 0 | - | - | - |
| | | 30 | a | - | - |
| | | 180 | a, b | a, b | - |
| | ***In vivo phosphorylated ERD14*** | | | | |
| **1. In the absence of Shrimp Alkaline Phosphatase** | | | | | |
| 43-55(II) | PEETPIASEFEQK | | a, b, c | - | - |
| 56-66(III) | VHISEPEPEVK | | a, c | - | - |
| 77-94(IV) | SDSSSSSSSEEEGSDGEK | | - | a, b | a, b, c |
| 104-111(V) | PTTEVEVK | | a, b, c | - | - |
| 168-174(VI) | LPGYHPK | | - | b | - |
| 175-181(VII) | TTVEEEK | | a, b, c | a, b, c | - |
| **2. In the presence of Shrimp Alkaline Phosphatase** | | | | | |
| 43-55(II) | PEETPIASEFEQK | | a | - | - |
| 56-66(III) | VHISEPEPEVK | | a, c | - | - |
| 77-94(IV) | SDSSSSSSSEEEGSDGEK | | - | - | - |
| 104-111(V) | PTTEVEVK | | a | - | - |
| 168-174(VI) | LPGYHPK | | - | b | - |
| 175-181(VII) | TTVEEEK | | a, c | a | - |

Appendix 4. MALDI-TOF/MS identification of the phospho-peptides in ERD14 (Alsheikh et al., 2003).

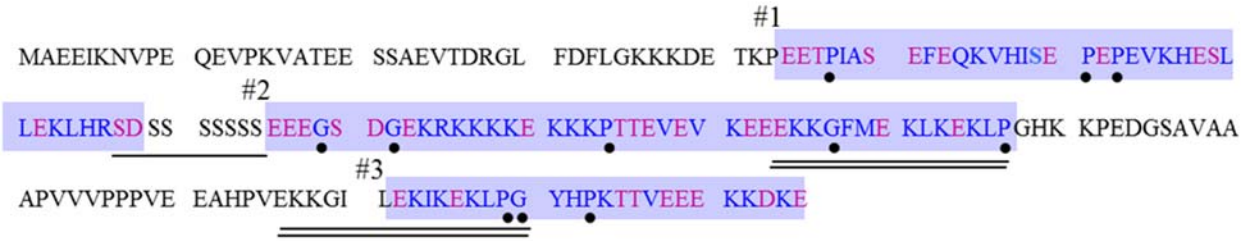


Appendix 5. ERD14 protein sequence. S-domain is single underlined, K-domains are double underlined, possible calcium binding domains (1, 2, or 3) are highlighted in blue, red letters indicate amino acids often involved in calcium-binding. Proline and glycines in putative calcium-binding domains are under-dotted.

```
ERD14_T3        MAEEIKNVPEQEVPKVATEESSAEVTDRGLFDFLGKKKDETKPEETPIASEFEQKVHISE
ERD14_T3.5      MAEEIKNVPEQEVPKVATEESSAEVTDRGLFDFLGKKKDETKPEETPIASEFEQKVHISE
ERD14_WT        MAEEIKNVPEQEVPKVATEESSAEVTDRGLFDFLGKKKDETKPEETPIASEFEQKVHISE
                ************************************************************

ERD14_T3        PEPEVKHESLLEKLHRSDSSSSSSSEEEGSDGEKRKKKKEKKKPTTEVEVKEEEKKGFME
ERD14_T3.5      PEPEVKHESLLEKLHRSDSSSSSSSEEEGSDGEKRKKKKEKKKPTTEVEVKEEEKKGFME
ERD14_WT        PEPEVKHESLLEKLHRSDSSSSSSSEEEGSDGEKRKKKKEKKKPTTEVEVKEEEKKGFME
                ************************************************************

ERD14_T3        KLKEKLPGEX----------------------------------------------------
ERD14_T3.5      KLKEKLPGE-----------------------------------------------------
ERD14_WT        KLKEKLPGHKKPEDGSAVAAAPVVVPPPVEEAHPVEKKGILEKIKEKLPGYHPKTTVEEE
                ********.

ERD14_T3        -----
ERD14_T3.5      -----
ERD14_WT        KKDKE
```

Appendix 6. Protein sequence alignment for ERD14 (WT), T3 and T3.5 truncation mutants comparing T3 and T3.5 sequence. T3 shows no significant difference in its protein sequence compared to T3.5 truncation mutant.

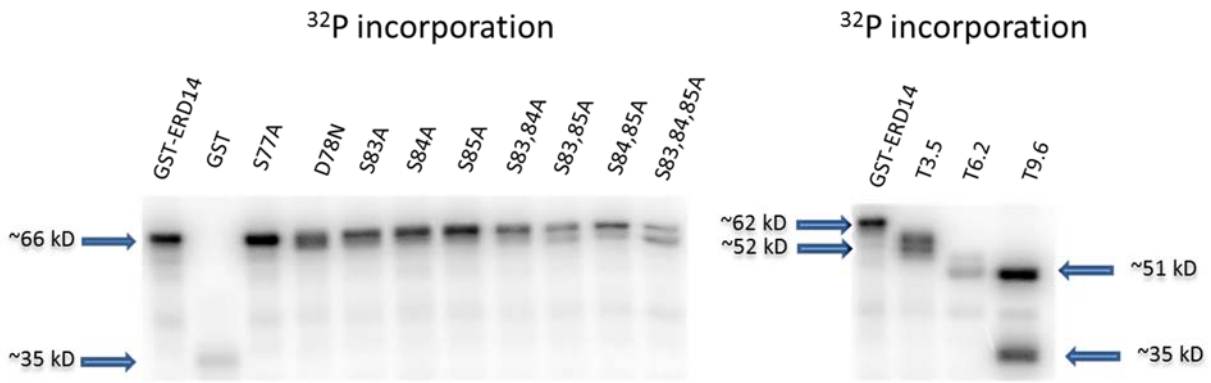


Appendix 7. Two hours $^{32}P$ incorporation kinase assay. E. coli-expressed GST-ERD14 (WT), GST, and S83,84,85A mutants were in vitro phosphorylated with CKII in the presence of [ɣ-32P]ATP for 2 h at 30°C.

VITA

VITA

**Allen Chacha**

**EDUCATION**

---

**Indiana University-Purdue University (IUPUI), Indianapolis, Indiana** December 2014

Masters of Science: Molecular Biology

**IUPUI, Indianapolis, Indiana** January 2012 – May 2012

Macro-economics, Micro-economics, Intro to accounting, Business statistics, Inorganic chemistry

**Butler University, Indianapolis, Indiana** August 2005 **-** May 2009

Bachelor of Science, Major: **Biology** Minor: **Chemistry**

**EXPERIENCE**

---

**Research Assistant - Master's thesis project**

IUPUI Biology department, Indianapolis, IN 08/2012 – 05/2014

Principal Investigator: Stephen Randall

*Investigated the relationship between phosphorylation and calcium binding activities on ERD14 dehydrin protein and their ability to confer cold tolerance in Arabidopsis thaliana plant, in-vivo and ex-vivo.*

- Designed and conducted experiments, analyzed data and developed solutions to technical problems associated with the characterization of ERD14 dehydrin protein in *Arabidopsis thaliana*.
- Extracted and characterized DNA and proteins from plant samples using standard cellular, molecular and biochemistry techniques such as plasmid prep, sterile tissues cell culture techniques, DNA isolation and sequencing, expression analysis, kinase assays, Westerns, Southerns, protein quantification, and PCR.
- Worked with radioisotopes ($^{32}$P & $^{45}$CA), chemical and biological hazards.
- Wrote and reviewed protocols, wrote study reports and presented data to peers and teachers.
- Presented at the 129$^{th}$ annual Indiana academy of science meeting in March 2014.

**Teaching Assistant - Introduction to Biology and Genetics**

IUPUI Biology department, Indianapolis, IN 08/2012 – 05/2014

- Taught a class of 30+ students on basic biology concepts and laboratory techniques every semester.
- Utilized PowerPoint presentations and online resources to further assist students understand biology concepts applicable to their laboratory activities.
- Identified and recommended students who required extra assistance in mastering biological concepts.
- Provided feedback at semesters end to faculty on ways to improve to help students learn laboratory techniques and understand biology concepts better.

**Cell Biology Research Associate**

Dow AgroSciences, Indianapolis, IN 08/2009 – 12/2011

- Worked alongside a research scientist in canola, maize and tobacco plant cells transformation projects.
- Served as a two person team in successfully meeting a company milestone for canola gene targeting project and protocol optimization in 2010.
- Received employee recognition award in 2010 and 2011 for excellent work quality and outstanding research project management ability, meeting supervisor's company project goal while away from work.
- Provided input and active participation in project meetings and assist other team members with their projects whenever necessary.
- Independently documented work and maintained study documentation and laboratory records.
- Suggested and performed modifications on methods or procedures where necessary to improve our project efficiency.

**Research Assistant - Environmental Chemistry**

Butler University - Professor Olijude Akinbo, Indianapolis, IN 01/2009 - 05/2009

*Investigated heavy metal concentrations in four potato chip brands from companies that produced baked and fried potato chips, consumed by Butler university students regularly.*

- Prepared a research grant.
- Prepared sample digestions, instrument and sample calibrations, and utilized LC/MS analysis techniques.
- Performed basic LC/MS instrument maintenance, troubleshooting, and repair.

**Research Assistant – Chemistry Independent study**

Butler University - Professor Joseph Kirsch, Indianapolis, IN 05/2007 – 05/2008

*Investigated the changes in secondary structure of apo and holo-transferrin protein in water using infrared spectroscopy resulting from the treatment with alcohols of different R-group sizes.*

- Gave a poster presentation at Evansville University, chemistry seminar in fall 2008.
- Gave an oral presentation of my research to students and academics from various Indiana universities at the Butler University Undergraduate Research Conference (URC) in fall 2008.

**LEADERSHIP**

---

**Mentor**, College Mentors For Kids (CMFK) Fall 2008 - 2009

**Secretary**, Butler University Pre-Health organization Fall 2007 – 2008

**Vice president**, Butler University International club Fall 2006 – 2008

**Diversity Co-Chair**, Butler University Student Government (REACH) Fall 2006 – 2007

**President**, Biology Graduate Organization Fall 2013 – 2014

**Organizer**, 2013 IUPUI Biology graduate school symposium Fall 2013